E-project-050107-122628

Grain Coarsening Behavior of two Gamma Prime (γ')

Ni-based Superalloys

A Major Qualifying Project Report

Submitted to the Faculty

of the

WORCESTER POLYTECHNIC INSTITUTE

in partial fulfillment of the requirements for the

Degree of Bachelor of Science

in Mechanical Engineering

by

Anthony George

Danielle Modeste

Daniel Waitt

Date: Thursday, April 26, 2007

Approved:

_____

Prof. Richard Sisson, Advisor

Keywords

1. Heat Treatment
2. Superalloy
3. IN100
4. Grain Growth

Abstract

The effect of heating rates on the grain growth kinetics of two wrought nickel-based superalloys (IN100 and N210) has been experimentally investigated. The specimens were heat treated through heat immersion and a heating rate of one degree per minute up to two temperatures above their respective solvus, 15 and 75 degrees Fahrenheit and held there for 15 and 120 minutes. It was found that the grain growth kinetics were faster for the samples that underwent the slower heat rate.

Acknowledgements

We have been very privileged to work with devoted individuals throughout the course of this project. We would like to extend special thanks to Professor Sisson and Robert Grelotti their advice throughout the entire project. Additionally, we would like to thank Md. Maniruzzaman and Boquan Li for their continuous support throughout the project, in particular with sample preparation and image acquisition. We would also like to thank Toby Bergstrom for his expertise and knowledge of machining. Lastly, we would also like to thank Administrative Assistant Rita Shilansky.

Table of Contents

List of Figures

List of Tables

List of Equations

1 Introduction

Superalloys have been developed for high temperature application in jet engines (Decker, 1970). In a jet engine, the high temperature can lead to disk failure and it is necessary to find an appropriate material that will meet all the mechanical requirements. These disks are currently being made out of nickel-based superalloys because they are ideal for high and low temperature settings. These superalloys are comprised of nickel, aluminum, titanium, chromium, and several other elements that provide high temperature strength and oxidation resistance (Decker, 1970).

During service these alloys experience high temperature exposure that can modify the alloy's microstructure(Decker, 1970). These alloys are heat treated to produce the microstructure to develop specified precipitates that prevent those modifications occurring during service. A superalloy's chemical composition in heat treatment can be modified to develop the microstructure to achieve the desired properties. Using this technique it is important to examine the microstructure of the metal because grain size has a significant impact on key design properties. One affect could be that the finer grains produce a more brittle material (Callister, 2007). By studying the effects of different heat treatments on the microstructure of superalloys, it can be determined what further improvements, if any, can occur. The creation of a superalloy however is task specific and metallurgy helps solve many problems that industries have with mechanical properties as well as aesthetics.

Figure 1-1: Jet Engine Disk

This project focused on determining the effects of heat treatment on the microstructure of two superalloys; IN-100 and an experimental nickel-based superalloy N-210. By applying selected heating rates, final temperatures, and dwell times an accurate analysis was done to determine the effects of heat treatment on grain size. Microstructural analysis was performed in order to determine the relationship between the temperature profile and the final grain size.

2 Background

Most materials wouldn't meet the requirements for jet engines especially because of the extreme temperatures of operation. Also, the metal has to be able to withstand multiple stresses while maintaining the pre-prescribed life cycle. A slight change in the composition of the superalloy can affect the properties and metallurgists are constantly testing new alloys to see which properties can be enhanced.

2.1 Superalloys

A superalloy is a high performance nickel alloy which is a combination of chromium, aluminum, titanium, cobalt, molybdenum, and iron (Pense, 2001). It is made to withstand extreme conditions. When first developed for jet aircrafts, they were made up of about only four or five elements that were age-hardened, but after some metallurgical developments, they also were solid-solution and precipitation hardened (Pense, 2001). The fact that superalloys are stronger than traditional alloys is due mainly to solid- solution strengthening which prohibits slip or dislocation motion. Precipitation hardening also helps the strength properties of alloys (Decker, 1970).

Aircraft engines require materials with good fatigue resistance, high modulus, and low density at elevated temperatures. Also, they strive to have 5,000-40,000 hour life which is directly correlated to high performance and reliability (Decker, 1970). Nickel-based superalloys are complex alloys and their properties are very well suited for jet engines. Nickel is used in many different engineering applications. It is ductile, tough, and has high oxidation and corrosion resistance at both high and low temperatures. When combined with other metals in a nickel-based alloy many of the properties are enhanced and this performance is mainly because of the addition elements such as niobium, zirconium, boron and iron.

There are many nickel-based superalloys, this experiment called for the use of IN-100 and N210. The material can change depending on the specific phase of the metals because at certain stages it can contain certain carbide and oxide forms. To create carbides, carbon reacts with different refractory elements that are present to form primary MC carbides. Examples of different carbides include $M_{23}C_6$ and M_6C (Decker, 1970). The carbide forms close to the grain boundary and since it is more brittle and harder than the alloy it prevents excess grain boundary sliding which can cause premature fracture. Carbides are the main reason for more enhanced

mechanical properties. They are the cause of reduced creep life, reduced ductility, increased rupture strength and the carbides aide in the chemical stability of the material by removing other reacting elements. The oxides protect the specific alloy from the environment.

During service the microstructure of these alloys will change at high temperatures. The grains grow. Precipitates may form or dissolve. The following sections of the report describe the kinetics of those transformations as well as the effects on mechanical properties.

2.2 Grain Size and Heat Treatment

The grain size has a significant affect on the properties of a material in particular the strength. Processing, chemistry and deleterious phases can affect grain coarsening. Equation 2-1 presents the relationship between yield strength and grain size (ASM Handbook Online,2003). σ_y represents yield strength, σ_i represents the stress related to the resistance of dislocation motion within a grain, c represents the parameter relating grain size strengthening, and d is the average grain diameter.

$$\sigma_y = \sigma_i + c/\sqrt{d}$$

Equation 2-1: Hall- Petch Equation

The average grain size was determined by equation 2-2 which describes grain growth in relation to the effective time of heat treating.

$$d^2 - d_0^{\,2} = kt_{effective}$$

Equation 2-2: Kinetics of grain growth equation

Generally in a superalloy the grain size increase is directly proportional to the increase in the rupture stress and creep resistance (Decker, 1970). This means that when the grains are too fine the creep and rupture stress are decreased.

The strengthening and growth of γ' [$Ni_3(Al,Ti)$] in grain coarsening blocks slip. Also, the solid solution in γ-Ni inside can block dislocation motion. However, there can be harmful precipitates in the microstructure that can negatively affect the performance of the material. Cellular carbides and σ phases are two undesirable phases (Decker, 1970). σ is formed due to the alloy chemistry and causes brittleness at low temperatures. The composition of σ is $(Cr, Mo)_x$ $(Ni, Co)_y$ where x and y vary from 1 to 7(Decker, 1970). By changing the specific heat treatment,

cellular carbides can be eliminated. However, to remove the σ phase it is necessary to create a completely different alloy by changing the compositions.

2.2.1 IN-100

The chemical composition of IN100 is presented from Figure 2-1(Pense, 2001). The solvus temperature, the temperature at which only γ-Ni is present, of IN-100 is 1463 Kelvin

Composition wt%						
Carbon	**Chromium**	**Molybdenum**	**Cobalt**	**Titanium**	**Aluminum**	**Boron**
0.18	10.00	3.00	15.00	3.00	5.50	0.014

Figure 2-1: Composition of IN100

(Grelotti, Robert). The material is classified as a no refractory disk alloy. Below 975 Kelvin the microstructure remains unchanged.

2.2.2 N210

The second material that was heat treated was N210, an experimental proprietary superalloy. The solvus temperature is 1470 Kelvin(Grelotti, Robert). This superalloy is a Pratt and Whitney experimental high refractory disk alloy. There were two forge temperatures for N210; N210-B which was forged at 1422 Kelvin and N210-D which was forged at 1338 Kelvin.

3 Methodology

The goal of this project was to investigate the behavior of grain coarsening relative to two temperatures 15 degrees and 75 degrees above solvus temperatures mentioned above as well as, determine the resulting grain size for two alloys IN 100, a non-refractory production high temperature disk alloy and N-210 a high-refractory production disk alloy. This chapter outlines the experimental methods used to determine the effects of temperature relative to the solvus temperature, heating rate through the solvus temperature, and soak duration on the grain coarsening behavior of two nickel based superalloys. In this chapter, the processes used for heat treatment was explained, specimen preparation, image acquisition, and specimen measurement and analysis.

3.1 Heat Treating

The following sections describe the methods used to heat treat each specimen; first how the temperature sensing sample was prepared then detail how temperature and time data was recorded for all of the samples. Also described in this section is the process of calibrating the furnace with respect to our thermocouple inside a drilled sample and how the furnace was programmed for the various heating rates, soak temperatures, and soak times. This procedure was outlined by Mohammed Maniruzzaman.

3.1.1 Temperature Recording Preparation

A sample that had an Omega KQIN-116G-24 Thermocouple in the geometric center to assist in recording temperature and time data was used. Two samples were prepared one IN100 with 1 x 1x 2 dimensions and one N210D with 1 x 1.5 x 2 dimensions, since the geometric shape and chemical composition of the two samples were different, and thus would affect heating rates. In each case, both samples were drilled to the geometric center using a 1/16" diameter titanium drill bit so that the thermocouples would fit securely inside the specimen.

3.1.2 Temperature and Time Data Acquisition

To acquire the temperature of the sample with respect to time, a Dell Inspiron 3800 notebook computer equipped with the LabVIEW virtual instrument program, National Instruments AI-16XE-50 Data Acquisition Card and National Instruments SCB-68 Shielded 68-Pin I/O Connector Block capable of acquiring temperatures readings from the particular type of

thermocouple, was used. The LabVIEW program had already been developed by a previous MQP team to measure temperature as a function of time (Guinn, 2006). The program was very intuitive, and allowed selection of the thermocouple channel, change the rate at which data is acquired, and save all time and temperature data to a file for later analysis.

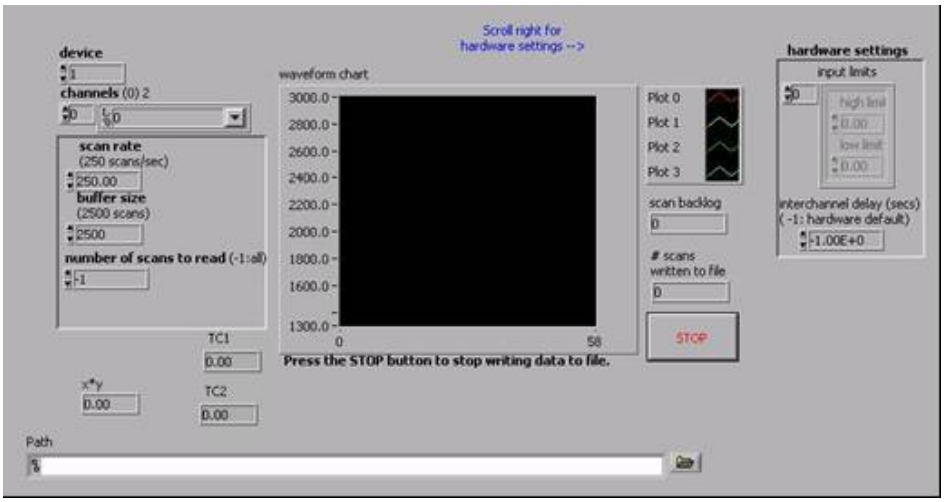

Figure 3-1: LabVIEW Front Panel

3.1.3 Furnace Calibration

Throughout all heat treatments, a Baker Model 6 Furnace with Honeywell Temperature Control Unit was used (Figure 3-7). High-conductivity free-machining copper, with a known melting point of 1340 to 1349 K, was melted in a crucible within the furnace in order to calibrate the furnace. The value was measured from the thermocouple inside the copper, and compared to the known melting temperature of this particular copper alloy. Figure 3-8 shows thermal arrest segment of the copper. It was established that the thermocouple in the copper was reading the correct melting temperature for the copper, an average of 1344 degrees

Figure 3-2: Baker Model 6 lab Furnace with Honeywell Temperature Control

Kelvin. This is a valid assumption because it falls within melting point of the high-conductivity free-machining copper. The furnace was offset by the appropriate amount of degrees at the given temperatures. In order to establish what temperature the furnace should be set to according to the heat treatment temperatures, the furnace was to the target temperatures as measured by the thermocouple inside our test sample. This reading was then compared to the thermocouple reading on the furnace display so that the furnace could later be set to the correct target temperature.

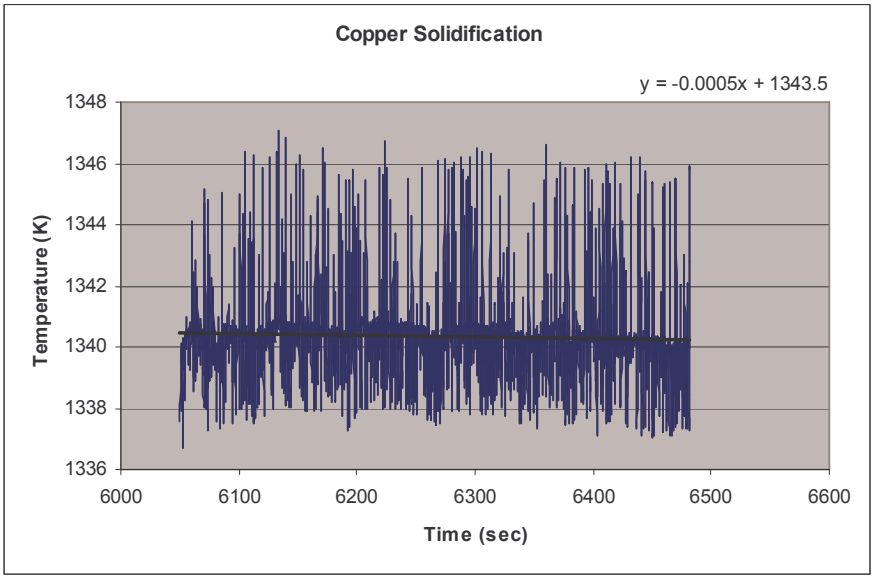

Figure 3-3: Temperature arrest segment of high-conductivity free-machining copper.

3.2 Sample Preparation

3.2.1 Cutting

After the samples had been heat treated, they were cut along their cross-section so that the desired microstructure could be photographed and analyzed. Using the Mark V CS600-A abrasive saw in conjunction with a 647 SiC blade each sample was sectioned the specimens and they later were mounted.

3.2.2 Mounting

All of the specimens were then mounted in Buehler phenolic powder using two Buehler LTD Simplimet II mounting machines. Instructions used for mounting the samples can be found in Appendix E.

3.2.3 Grinding and Polishing

The newly mounted samples were then put though a routine of grinding and polishing which was described in detail by Mohammed Maniruzzman. This process started at the manual Metaserv 2000 grinding / polishing machine shown in (Figure 3-3) where the samples were ground successively starting at 120 grit paper. After the scratches on the specimen were consistent throughout and there appeared to only one flat surface, the grit paper was exchanged for a finer grit paper. This process was repeated with 120, 240, 320, 400, and 600 grit papers. Once the grinding was completed, the samples were put into the Ultramet 2002 Sonic cleaner. The samples were immersed in acetone and ultrasonically cleaned for 5 minutes to remove any lose particulates left on the surface from the grinding process.

The freshly cleaned specimens were then polished using diamond polishing solution. The specimens first started with the 9 micron polishing solution which was used on an Ecomet 5 two -peed grinder / polisher. The solution consisted of 9 micron diamonds suspended in a distilled water-based solution. Before beginning polishing, the wheel was wet down and the diamond solution was added. The specimens were then polished until further polishing was not able to alter the specimen's surface. They were again cleaned by the Sonic Cleaner, similar to steps taken after grinding process. These steps were repeated by moving to the finer 6 micron diamond polishing solution, and then 3 micron solution. After the manual polishing had been completed, the last step involved using the Buehler I vibrating polisher. The samples were secured in small collets and placed faced down onto the automatic vibrating polishing machine. The samples were polished for approximately four hours using a 1 micron water based solution. The samples were then placed under an optical microscope to examine their surfaces and ensured that there were not any visible defects. Once it was determined that the sample's surface was properly ground and polished, the samples were ready for etching.

3.2.4 Etching

Etching can be described as a process of using a strong acid to reveal optically enhanced microstructural features. Kallings Waterless solutions was determined from a previous MQP team working with similar materials to provide the proper etching characteristics needed to observe the grain boundaries of our specimens. The solution that was prepared consisted of 100 mL of Methanol, 100 mL of Hydrochloric Acid, and 5 g of Copper Dichloride. Etching characteristics were tested on previously prepared practice samples. The samples were soaked in

the solution for 30 seconds at a time. After the 30 seconds the specimens were run under cold water to remove any remaining etchant, then washed with acetone and blown dry. In between soaks the newly etched surface was observed under an optical microscope to determine if the grain boundaries. It was found from the heat treated samples that etching times varied substantially. The samples took between 3 and 5 minutes before the grain boundaries became visible under an optical microscope. A new technique was also employed in which the samples were held by hand and suspended in the solution.

3.3 Image Acquisition and Microscopy

After the specimens had been heat treated, cut, mounted ground, polished, and etched, images were taken using an optical microscope. The magnification had to be adjusted to produce an image of good quality for which further analysis could take place.

To obtain optical images of our specimens, a Nikon Epiphot optical microscope was used in conjunction with a Nikon Digital Sight DS-U1 camera. The program used to capture the images was ACT-2U. Within this program, the contrast, focal point and resolution were adjusted to achieve optimal photographs. This program also had the ability of placing a user created scale onto the image for later analysis. All of the images taken were saved onto the computer and used in later analysis. An optical photomicrograph of sample 10B is presented in Figure 3-3.

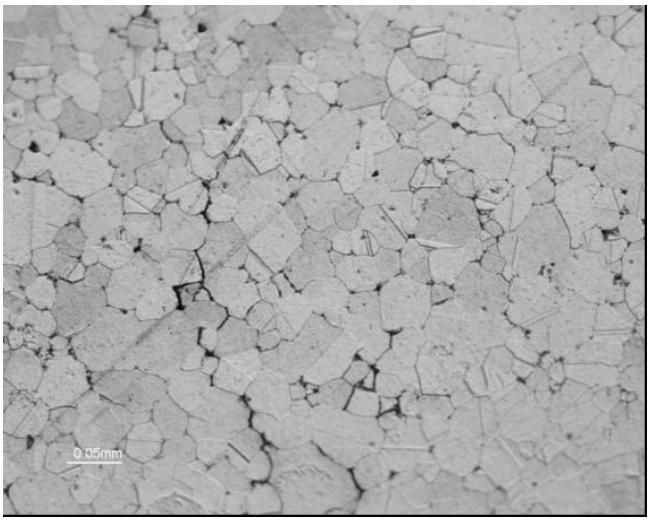

Figure 3-4: Photo-micrograph of sample 10B.

3.4 Measurement and Analysis

In this section, the processes used to measure the grain size of the specimens are described. First, the linear intercept method was used to find the average grain diameter. Next, with the aid of a special ASTM Austenite grain size graticule, the ASTM grain size of each sample was measured using the same Nikon Epiphot optical imaging microscope used to take the photo-micrographs.

3.4.1 Average Grain Diameter

To measure the average grain diameter of each sample several images of each specimen were printed. Each group member received one image of each specimen. These images were taken at different locations on the specimen so that the average grain diameter of the entire specimen could be evaluated. On each printed image, 5 lines were drawn 4.7 cm long and the number of grains that were intercepted by each line was counted. All of the data was collected by each team member and was averaged together accordingly. Then using an equation 3-1 (Callister, 2007), the average grain diameter was calculated. An example of this process is shown in Figure 3.5 and is accompanied by sample results in Table 3.1.

$$d = \frac{C}{n_L \times m}$$

Equation 3-1: Average grain diameter equation

Line	Intercepts
1	7
2	5
3	5
4	9
5	6
Average	6.4

Line Length (mm)	47.8
Grains/cm	0.13
Magnification	240
Constant C	1.5
Grain Diameter (mm)	0.0459

Table 3-1: Sample linear intercept calculations

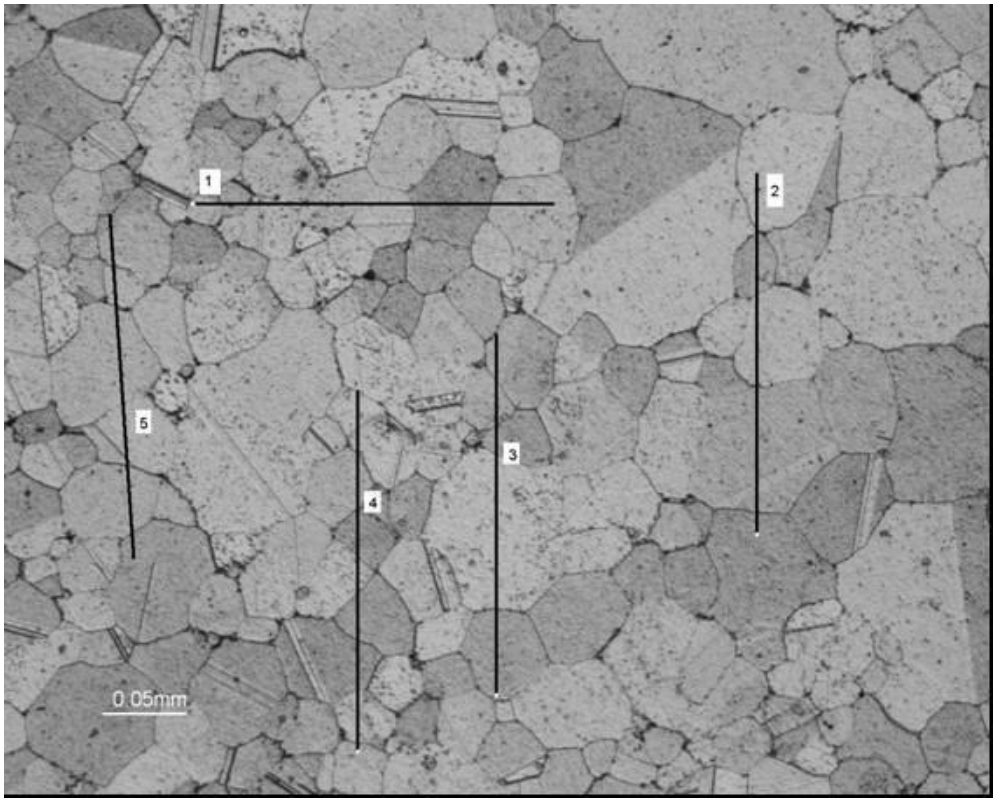

Figure 3-5: Grain Intercept Method

3.4.2 ASTM Grain Size

Measuring the ASTM grain size of each sample entailed using the Nikon Epiphot optical microscope. Using an ASTM Austenite grain size graticule the specimens were manually viewed and the ASTM grain number of the specimen was determined by matching the grains in the images to sizes given on the graticule. An image of the grain graticule can be found in Figure 3-7.

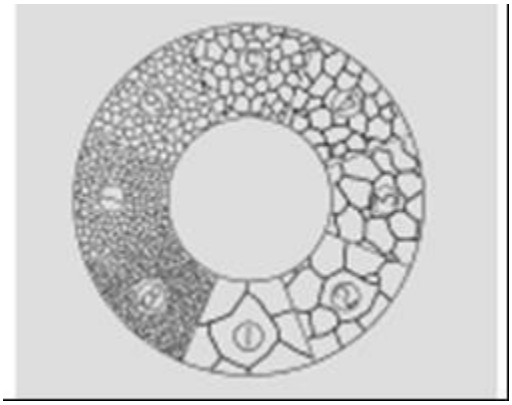

Figure 3-6: Details Austenitic Grain Graticule

4 Experimental Plan

The furnace that was used allowed us to set the desired heating rates, temperatures, and soak durations. Our experimental heating matrix is below in Table 3-1. For heat immersion, setting the temperature was very straight forward. From the furnace calibration, the furnace was set to the temperature which was achieved by the desired thermocouple reading. Using our thermocouple equipped sample, time and temperature data were acquired once the furnace was up to temperature. The furnace temperature varied as the heating element turned on and off, so the temperature was first evaluated during three up and down heating cycles. It was noticed that during this time the variations in temperature were around 400 degrees and it was evaluated that this was the result of electrical noise produced by the heating element of the furnace. The average of the temperature data was taken to ensure that approximately the correct temperatures were achieved. This process was repeated for each heat immersion sample. The furnace was quickly opened to prevent substantial heat loss, and the sample was set into the furnace next to the thermocouple sample to ensure that the heating effect would be similar. The IN100 samples were heat treated independently, but both N210 forgings, B (1422K) and D (1338K), were placed in the furnace at the same time. Once the samples had soaked for the desired amount of time, they were taken out of the furnace and immediately quenched in ice water to lock in the microstructure.

Heating Matrix								
IN100					**N210**			
Heat Rate: Immersion		Tempurature	Tempurature		Heat Rate: Immersion		Tempurature	Tempurature
		2190 F	2250 F				2203 F	2263 F
Soak Duration	15 min	1	2		Soak Duration	15 min	9	10
Soak Duration	120 min	3	4		Soak Duration	120 min	11	12
Heat Rate: 1 degree / min		Tempurature	Tempurature		Heat Rate: 1 degree / min		Tempurature	Tempurature
		2190 F	2250 F				2203 F	2263 F
Soak Duration	15 min	5	6		Soak Duration	15 min	13	14
Soak Duration	120 min	7	8		Soak Duration	120 min	15	16

Table 4-1: Heating Matrix

Because the copper specimen was relied on to report the temperature of the furnace before the actual samples were placed inside, the heating effects of immersing our specimens into a hot furnace had to be determined. The furnace was heated up to the same temperature used for the various heat treatments, then the thermocouple sample was placed into the furnace and the temperature and time data was measured up until the sample reached the desired

temperature. These data were later added onto the respective temperature and time data that was recorded during the actual heat treatments.

Using the previously gathered calibration data concerning the correct settings for the furnace, Individual programs were set up for the "heat rate" samples. The desired one degree per min heating rate, correct soak temperature and soak time were incorporated into each program. Each heat rate sample was placed in the furnace at a temperature between 1300 F and 1400 F because there would be no mircostructural changes taking place until the proper heating temperature was achieved (Grelotti, Robert). Similarly to the methods used in heat immersion, the samples were quickly placed into the furnace without losing a substantial amount of heat. After the samples had gone through the 14 to 16 hour heat treating cycle, they were taken out and immediately quenched into ice water. A check sheet was made to monitor the progress of each sample through the preparation process. Table 3-2 shows the preparation matrix used for each sample.

				Grinding							Polishing			1 Micron Machine			
Sample	Heat	Cut	Mount	60	120	180	240	320	400	600	9 micron	6 micron	3 micron	1 hour	2 hour	3 h	4 h
1																	
2																	
3																	
4																	
5																	
6																	
7																	
8																	
9B																	
9D																	
10B																	
10D																	
11B																	
11D																	
12B																	
12D																	
13B																	
13D																	
14B																	
14D																	
15B																	
15D																	
16B																	
16D																	

Table 4-2: Sample Preparation Matrix

5 Experimental Results

Here are two examples of the temperature time curves.

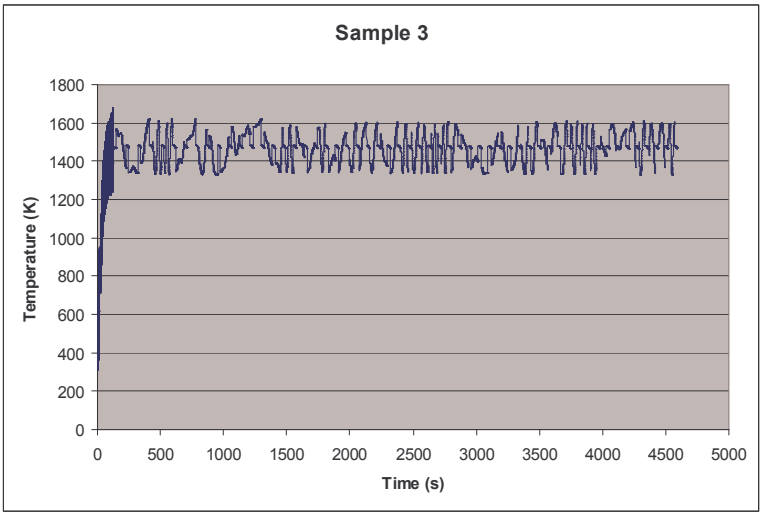

Figure 5-1: Temperature time curve for sample 3.

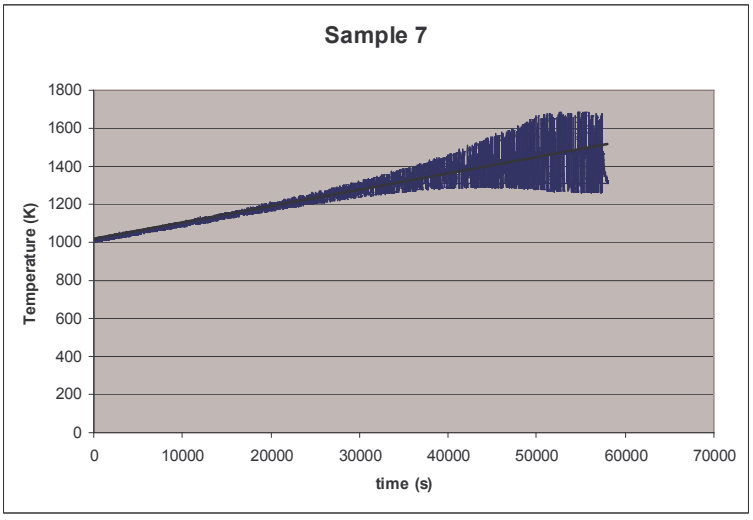

Figure 5-2: Temperature time curve for sample 7.

5.1 Measurement and Analysis

Multiple methods were used to measure the grain size. The first method involved the linear intercept method and manual calculations. The other two methods were both done using computer software. Also mathematical techniques were used to better define the grain behavior.

5.1.1 Average Grain Diameter

The average grain diameter was determined by using the procedure outlined in section 3.3.1. Table 5-1 displays the average grain diameter that was calculated for each sample, and several plots were made to analyze the grain growth.

IN100		N210B		N210D	
Sample	Grain Size (mm)	Sample	Grain Size (mm)	Sample	Grain Size (mm)
1	0.034	9b	0.034	9d	0.016
2	0.035	10b	0.047	10d	0.049
3	0.029	11b	0.042	11d	0.047
4	0.039	12b	0.061	12d	0.077
5	0.036	13b	0.038	13d	0.043
6	0.040	14b	0.053	14d	0.066
7	0.040	15b	0.047	15d	0.049
8	0.045	16b	0.090	16d	0.095

Table 5-1: Average Grain Diameter

For IN100 the grain diameter grew as the heating increased. For the N210 samples, the results match what is expected of heat treated metals. The grain diameter grew as the time lengthened and as the temperatures increased.

5.2 ASTM Grain Size

A graticule was used to find the ASTM grain number. These were observed manually using the optical microscope that was used in image acquisition. Table 5-2 shows the results of this measurement accompanied by the percent difference. On average the ASTM equivalent grain diameters differed from the measurements using the linear intercept technique by approximately 14%, which appears to be reasonable.

Sample	ASTM #	ASTM Equiv. Diameter (mm)	Linear Grain Diameter (mm)	% Difference
1	7.00	0.028	0.034	18.95
2	7.00	0.028	0.035	21.66
3	6.50	0.032	0.029	9.66
4	6.00	0.038	0.039	3.50
5	6.00	0.038	0.036	4.44
6	5.50	0.048	0.040	18.71
7	6.00	0.043	0.040	5.56
8	5.00	0.055	0.045	22.66
9b	6.00	0.038	0.034	11.94
9d	8.00	0.019	0.016	17.79
10b	6.00	0.038	0.047	19.58
10d	6.00	0.038	0.049	23.69
11b	6.00	0.038	0.042	10.78
11d	6.00	0.038	0.047	19.61
12b	5.25	0.050	0.061	17.41
12d	4.75	0.060	0.077	22.29
13b	6.75	0.033	0.038	13.91
13d	6.25	0.038	0.043	12.17
14b	5.25	0.053	0.053	1.28
14d	4.75	0.060	0.066	8.95
15b	6.00	0.040	0.047	14.85
15d	4.50	0.063	0.049	26.67
16b	3.75	0.088	0.090	3.30
16d	3.00	0.103	0.095	7.56
			Average % Diff.	14.04

Table 5-2: ASTM Equivalent Diameter Table

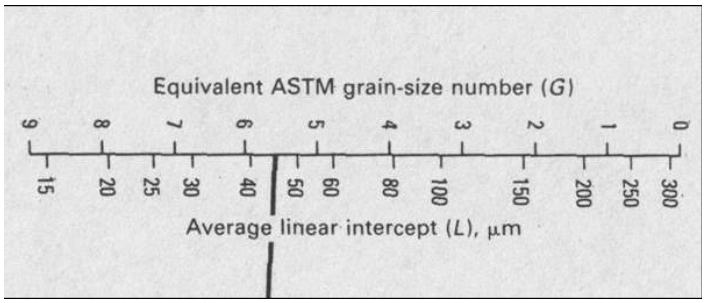

Figure 5-3: Equivalent ASTM Grain-size scale

By using the scale in Figure 5-1, equivalent grain diameter was found. This served as a basic comparison for the average grain diameter results.

5.2.1 Effective Time

For each sample the effective heating time was calculated. By finding the effective time, one can find how long the samples would need to be heated if they were soaked at the given temperature. The process to calculate effective time required using equations 5-1 and 5-2. The

first step in solving for the effective time was to create plots of Temperature versus Time. Next we calculated values for each sample using equation 5-3.

$$d^2 - d_0^{\ 2} = kT$$

Equation 5-1: Grain Growth Equation

$$t_{effective} = \frac{(A_1)}{e^{-Q/RT_{Soak}}}$$

Equation 5-2: Effective Time

$$k = k_0 e^{-\frac{Q}{RT}}$$

Equation 5-3: Exponential Law relating energy to temperature

$e^{-\frac{Q}{RT}}$ in equation 5-3 was plotted versus time and the MS Excel's trend-line feature was used to generate a best fit line. This gave us a good approximation of the data. A_1 is the area under the curve and was solved for by integrating the trend-line. The integration was done using Maple 10 to simplify our work which can be found in Appendix A.

Sample	Heat Rate	Soak Temp (F)	Soak Time (min)	Additional Eff. Time (min)	Total Eff. Time (min)
1	Immersion	2190	15	2.16	17.16
2	Immersion	2250	15	1.27	16.27
3	Immersion	2190	120	2.16	122.16
4	Immersion	2250	120	1.27	121.27
5	1 deg/min	2190	15	170.23	185.23
6	1 deg/min	2250	15	117.74	132.74
7	1 deg/min	2190	120	154.12	274.12
8	1 deg/min	2250	120	147.13	267.13
9b	Immersion	2203	15	2.11	17.11
9d	Immersion	2203	15	2.11	17.11
10b	Immersion	2263	15	1.91	16.91
10d	Immersion	2263	15	1.91	16.91
11b	Immersion	2203	120	2.11	122.11
11d	Immersion	2203	120	2.11	122.11
12b	Immersion	2263	120	1.91	121.91
12d	Immersion	2263	120	1.91	121.91
13b	1 deg/min	2203	15	189.06	204.06
13d	1 deg/min	2203	15	189.06	204.06
14b	1 deg/min	2263	15	239.32	254.32
14d	1 deg/min	2263	15	239.32	254.32
15b	1 deg/min	2203	120	174.50	294.50
15d	1 deg/min	2203	120	174.50	294.50
16b	1 deg/min	2263	120	286.82	406.82
16d	1 deg/min	2263	120	286.12	406.12

Table 5-3: Effective Time Table

The times were calculated in seconds and then converted to minutes for convenience.

Table 5-3 is the result of our effective time analysis. It can easily be seen that the effective times were much shorter for the samples that were placed in the furnace at their soak temperatures. The additional effective time column represents the time it would take for the sample to come up to temperature. The total effective time is the soak time plus the additional effective time.

Once all the effective times were calculated, grain diameter squared versus total effective time was plotted. By creating these the plots the diffusivity constant, k, for each sample was determined. The value of k is the slope of each of our trend-lines given in two examples of the grain diameter squared versus effective time charts (please see appendix B for the rest of the charts).

Samples	Temperature (K)	k (mm^2/min)	d_0(mm)
1 and 3	1472	-2.726E-06	0.0346
2 and 4	1505	2.648E-06	0.0345
5 and 7	1472	3.733E-06	0.0244
6 and 8	1505	3.046E-06	0.0346
9b and 11b	1479	6.138E-06	0.0319
9d and 11d	1479	1.824E-05	0.0072
10b and 12b	1513	1.420E-05	0.0440
10d and 12d	1513	3.378E-05	0.0429
13b and 15b	1479	8.644E-06	0.0184
13d and 15d	1479	6.765E-06	0.0210
14b and 16b	1513	3.515E-05	0.0782
14d and 16d	1513	3.122E-05	0.0600

Table 5-4: Table of experimental k and d_0 values

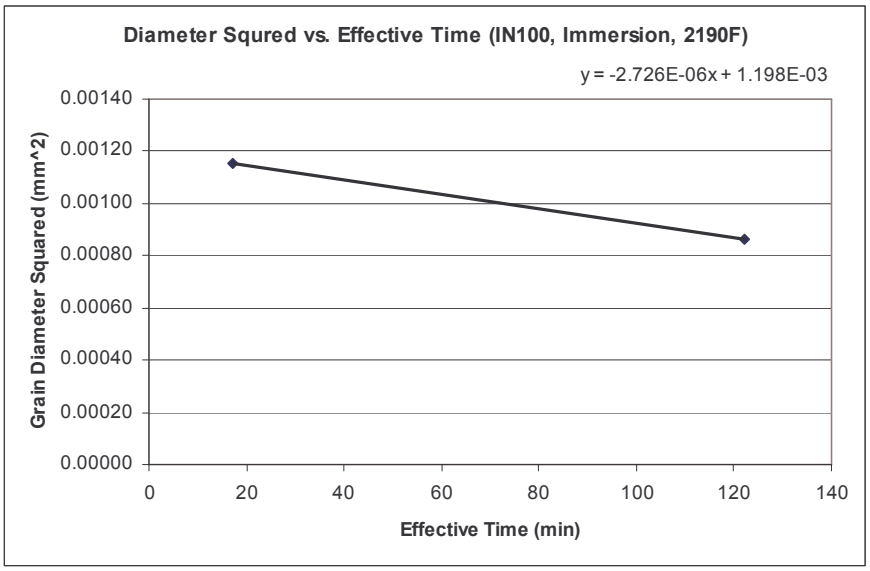

Figure 5-4: Diameter Squared vs. Effective Time (Samples 1 and 3)

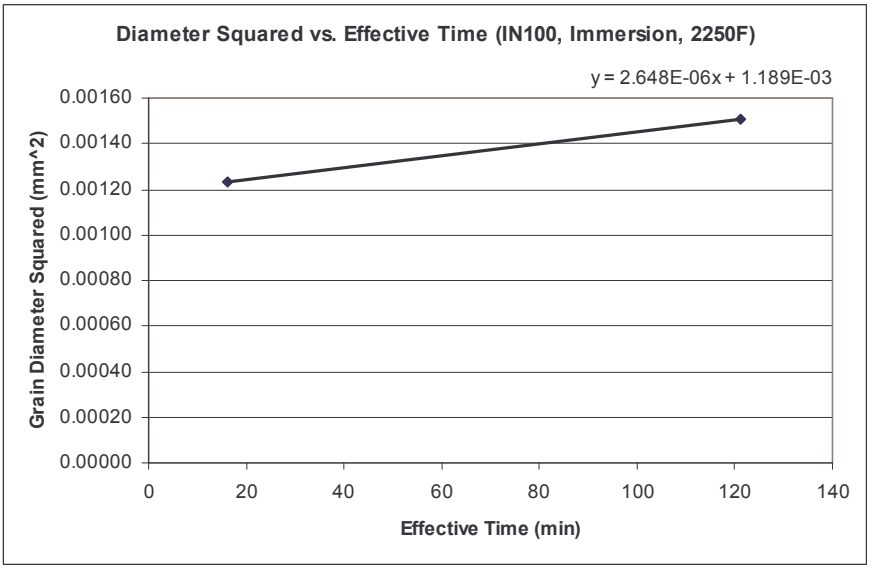

Figure 5-5: Diameter Squared vs. Effective Time (Samples 2 and 4)

6 Conclusion and Recommendations

The preparation procedure outlined at the start of the project worked well. There were relatively few problems over the course of the project. Some corrections were made however and they are discussed in this chapter.

6.1 Specimen Preparation

After several SiC blades were broken on the Mark V CS600-A saw, The technique used cut the samples was altered. Initially only a little pressure was exerted from the blade onto the specimen. However, this lead to inconsistent blade pressure, blade deformation, and thus fractured blades. After consulting with our project advisors, it was decided that the best way to cut the material was to allow the weight of the sample and holding-vice to rest on the cutting surface of the blade. This new technique not only resulted in lower cutting times, but also assisted in longer blade life.

There were very few problems with the mounted samples, and for the most part their overall size was consistent. The outlined procedure for mounting, found in Appendix E worked exceptionally well so there were no alterations necessary to the mounting procedure. After being cut and mounted, each sample underwent a long grinding and polishing process. Practicing this process before the project began was beneficial.

One observation that was made while grinding and polishing was that it was easier to grind and polish samples that had thicker mounts because they were easier to hold. The smaller samples were sometimes difficult to grind because it was tough to keep a solid grip to ensure even grinding. Also some of the samples had large burs from the cutting process. Those samples that had large defects or scratches were started using the 60 grit paper to help shorten the amount of time spent grinding. It also made it easier to form one flat surface using such a heavy grit paper. Another useful technique that was found was to rotate the sample 90° before beginning the next smallest grit paper. Using this technique, it was easy to determine if the sample was ready for the next size grit paper by observing the scratches. If the scratches from the paper appeared to all be in the same direction, the next paper would be used. This rotating of the samples made it more difficult to preserve one flat surface, but with practice it shortened the time spent grinding / polishing considerably.

The etching process was refined during the experiment. Better results were achieved when the specimens were suspended and gently agitated, rather than resting on the bottom of the dish. Using this technique, the etching also took less time. This was because the agitation sped up the chemical reaction occurring at the specimen's surface.

6.2 Grain Size

There were two methods used to solve for the average grain diameter of our specimens. The first method used was the linear intercept method to obtain the average grain diameter of our specimens. The second method was using the ASTM grain number approach. The Kallings etching solution gave us fairly consistent results. The grain boundaries were crisp and clear for most of our samples, which gave us accurate results.

The linear intercept method that was used involved manual calculations. The method was easy to understand and learn. It also wasn't very time consuming. The process was shortened by the use of Microsoft Excel. The average grain diameters increased with time and temperature as was expected.

The ASTM grain number approach was not as a precise process as the linear intercept method. However our results appear to be correct agree with the previously calculated grain diameters. The scale displayed in Figure 4.1.1-1 allowed comparison of the grain size results with the ASTM number. The similarity in values for each sample shows that the linear intercept calculations were accurate.

6.3 Effective Time

The effective time calculations were the most involved portion of the project for our group. However, after some trial and error, the effective times for each sample were solved for. Table 5-3 lists the results of our calculations. The heat immersion effective times were much shorter than the times for the 1 degree per minute samples. Since the grain growth took longer in heat rate samples, the effective times were much longer.

For each sample the experimental diffusivity constant, k was also calculated. These values were found by using the trend-line feature in MS Excel. This constant represents the rate at which grains grow in the samples with respect to time. The values for k were all fairly similar to each other, mostly falling between 1 and 10 microns squared per minute. The original grain size was also determined from the diameter squared versus effective time plots for example

Figures 5-5 and 5-6. The original grain diameter, d_0, is also determined by the graphs by taking the square root of the y-intercept for each plot.

6.4 Effects of Heating Rate on Grain Growth Kinetics

The table below displays k and d_0 values for the specimens. It can be seen that compared to the heating rate samples, grain growth kinetics for heat immersion was slower. All of the initial diameter (d_0) values for IN100 are similar however for N210 samples the values varied significantly.

	Heating	Temperature (K)	k (mm^2/min)	d_0(mm)
IN 100	Immersion 2190	1472	-2.726E-06	0.0346
	1 deg/min 2190	1472	3.733E-06	0.0244
	Immersion 2250	1505	2.648E-06	0.0345
	1 deg/min 2250	1505	3.046E-06	0.0346
N210B	Immersion 2203	1479	6.138E-06	0.0319
	1 deg/min 2203	1479	8.644E-06	0.0184
	Immersion 2263	1513	1.420E-05	0.0440
	1 deg/min 2263	1513	3.515E-05	0.0782
N210D	Immersion 2203	1479	1.824E-05	0.0072
	1 deg/min 2203	1479	6.765E-06	0.0210
	Immersion 2263	1513	3.378E-05	0.0429
	1 deg/min 2263	1513	3.122E-05	0.0600

Table 6-1: Comparison Chart of k and d_0

7 References

(2003). ASM Materials Information . Retrieved April 20, 2007, from ASM Handbook Online Web site: http://products.asminternational.org/hbk/index.jsp

(2003). Electron Microscopy Sciences. Retrieved April, 20, 2007, from emsdiasum.com Web site: http://www.emsdiasum.com/microscopy/products/magnifier/images2/g41.gif

(2006). Engineering Materials. Retrieved April 20, 2007, from Grain Size Conversion Web site: http://emat.eng.hmc.edu/database/grain_size_conversion.htm

Decker, R., & Sims, C. (1970). *Chapter 2: The Metallurgy of Nickel-Base Alloys*.New York:

Guinn, W., & Herchenroder, K. (2006). *Automate Image Analysis Routines for Recording Mircrostructural Features of IN100*.

Pense, A., & Brick , R. (2001). *and Properties of Engineering Materials: Fourth Edition*.New York: McGraw-Hill Book Company.

Smith, W. (1993). *Structure and Properties of Engineering Alloys: Second Edition*.New York: McGraw-Hill Book Company.

Callister, William D. Jr. (2007). *Materials Science and Engineering: An Introduction- 7th Edition*. York: John Wiley & Sons, Inc.,

8 Appendix

8.1 Appendix A: Maple 10 Worksheet

```
with(student);
```
[D, Diff, Doubleint, Int, Limit, Lineint, Product, Sum, Tripleint, changevar, completesquare, distance, equate, integrand, intercept, intparts, leftbox, leftsum, makeproc, middlebox, middlesum, midpoint, powsubs, rightbox, rightsum, showtangent, simpson, slope, summand, trapezoid] (1)

```
with(plots);
```
[Interactive, animate, animate3d, animatecurve, arrow, changecoords, complexplot, complexplot3d, conformal, conformal3d, contourplot, contourplot3d, coordplot, coordplot3d, cylinderplot, densityplot, display, display3d, fieldplot, fieldplot3d, gradplot, gradplot3d, graphplot3d, implicitplot, implicitplot3d, inequal, interactive, interactiveparams, listcontplot, listcontplot3d, listdensityplot, listplot, listplot3d, loglogplot, logplot, matrixplot, multiple, odeplot, pareto, plotcompare, pointplot, pointplot3d, polarplot, polygonplot, polygonplot3d, polyhedra_supported, polyhedraplot, replot, rootlocus, semilogplot, setoptions, setoptions3d, spacecurve, sparsematrixplot, sphereplot, surfdata, textplot, textplot3d, tubeplot] (2)

Sample 1 and 3

```
f := x → 1·10^(−10)·e^(.0004·x);
```
$$x \to \frac{1}{10000000000}\, e^{(0.0004\,x)} \tag{3}$$

```
plot((f(x)), x = −10..142);
```

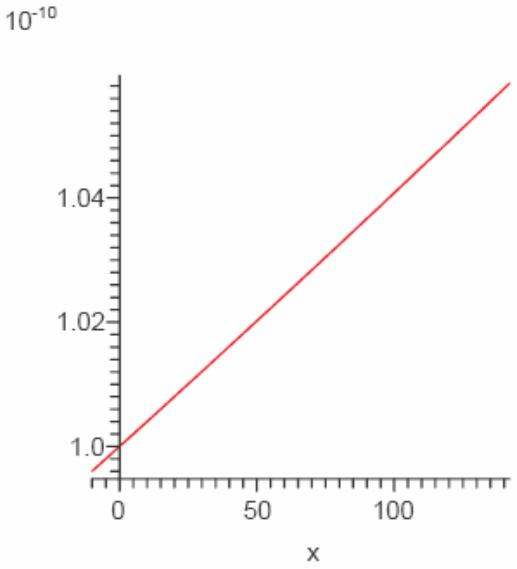

$evalf(int(f(x), x = 0..142));$

$$1.461102510\ 10^{-8} \quad (4)$$

$evalf\left(e^{-\frac{67000}{1.987 \cdot 1472}}\right);$

$$1.126147978\ 10^{-10} \quad (5)$$

$evalf\left(\frac{1.461102510\ 10^{-8}}{1.126147978\ 10^{-10}}\right);$

$$129.7433853 \quad (6)$$

Sample 2 and 4

$f := x \rightarrow 1 \cdot 10^{-10} \cdot e^{.0002 \cdot x};$

$$x \rightarrow \frac{1}{10000000000}\, e^{(0.0002x)} \quad (7)$$

$plot((f(x)),\ x=-10..140);$

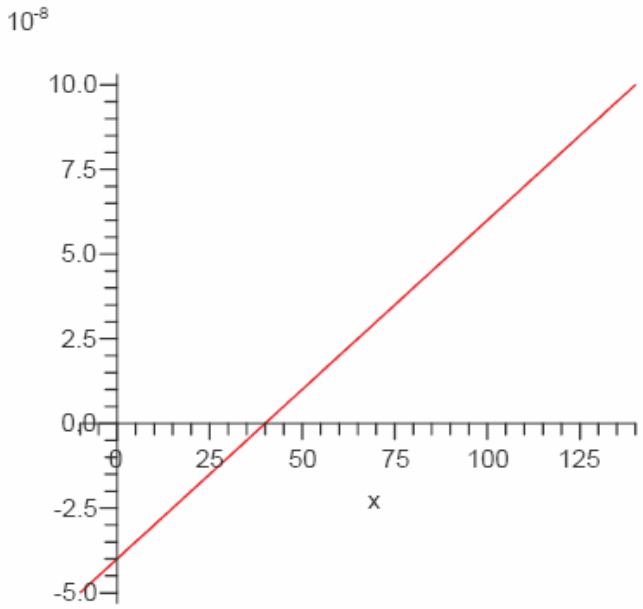

$evalf(int(f(x), x=0..140));$

$$1.419784221\ 10^{-8} \tag{8}$$

$evalf\left(e^{-\frac{67000}{1.987\cdot 1505}}\right);$

$$1.860943710\ 10^{-10} \tag{9}$$

$evalf\left(\frac{1.419784221\ 10^{-8}}{1.860943710\ 10^{-10}}\right);$

$$76.29377575 \tag{10}$$

Sample 5

$f := x \rightarrow 7\cdot 10^{-15}\cdot e^{.0002\cdot x};$

$$x \rightarrow \frac{7}{1000000000000000}\ e^{(0.0002x)} \tag{11}$$

$plot((f(x)),\ x=-10..52000);$

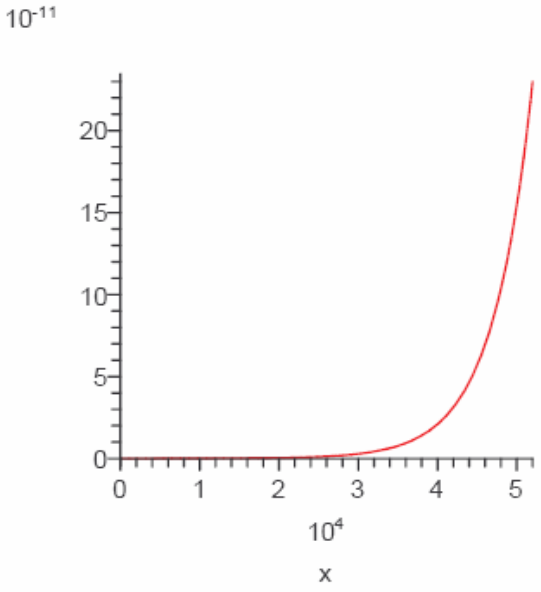

$evalf(int(f(x), x=0..52000));$

$$0.000001150051899 \quad (12)$$

$evalf\left(e^{-\frac{67000}{1.987\cdot 1472}}\right);$

$$1.126147978\ 10^{-10} \quad (13)$$

$evalf\left(\frac{0.000001150051899}{1.126147978\ 10^{-10}}\right);$

$$10212.26270 \quad (14)$$

Sample 6

$f := x \rightarrow 8\cdot 10^{-15}\cdot e^{.0002\cdot x};$

$$x \rightarrow \frac{1}{125000000000000}\, e^{(0.0002x)} \quad (15)$$

$plot((f(x)),\ x=-10..52000);$

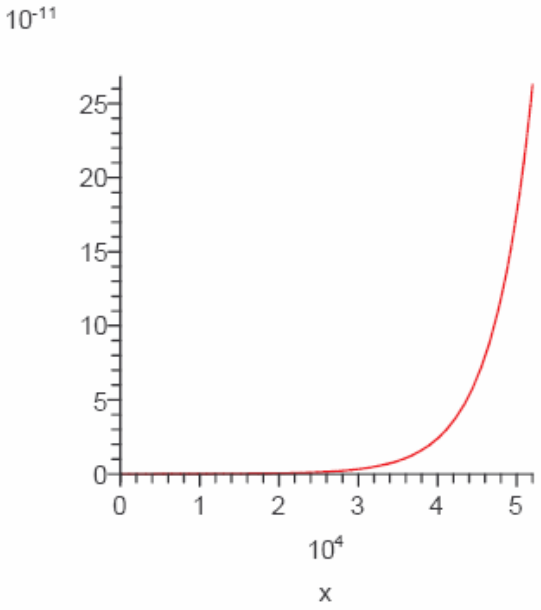

$evalf(int(f(x), x=0..52000));$

$$0.000001314345027 \tag{16}$$

$evalf\left(e^{-\frac{67000}{1.987\cdot 1505}}\right);$

$$1.860943710\ 10^{-10} \tag{17}$$

$evalf\left(\frac{0.000001314345027}{1.860943710\ 10^{-10}}\right);$

$$7062.787659 \tag{18}$$

Sample 7

$f := x \rightarrow 7\cdot 10^{-15}\cdot e^{.0002\cdot x};$

$$x \rightarrow \frac{7}{1000000000000000}\ e^{(0.0002x)} \tag{19}$$

$plot((f(x)),\ x=-10..52000);$

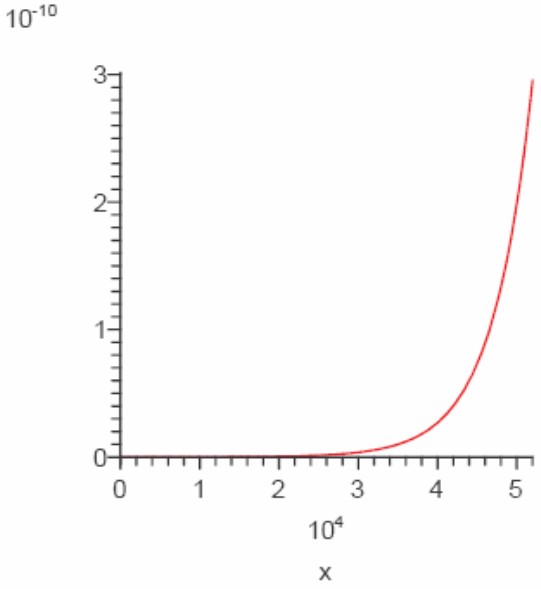

$evalf(int(f(x), x = 0..51500));$

$$0.000001040606660 \tag{20}$$

$evalf\left(e^{-\frac{67000}{1.987 \cdot 1472}}\right);$

$$1.126147978\ 10^{-10} \tag{21}$$

$evalf\left(\frac{0.000001040606660}{1.126147978\ 10^{-10}}\right);$

$$9240.407836 \tag{22}$$

Sample 8

$f := x \rightarrow 1 \cdot 10^{-14} \cdot e^{.0002 \cdot x};$

$$x \rightarrow \frac{1}{100000000000000}\ e^{(0.0002x)} \tag{23}$$

$plot((f(x)),\ x = -10..52000);$

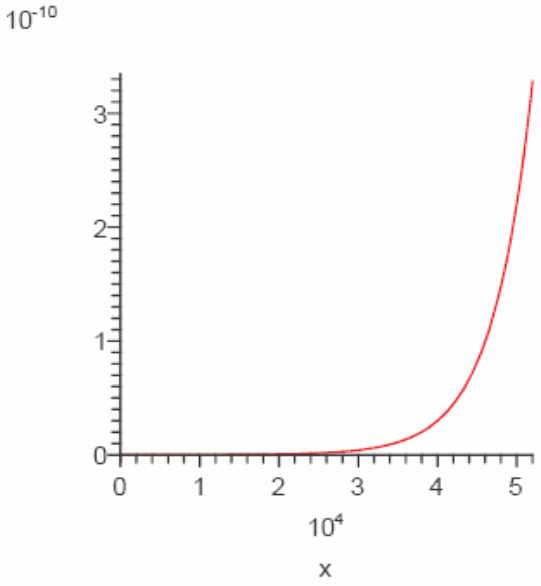

$evalf(int(f(x), x = 0..52000));$

0.000001642931284 (24)

$evalf\left(e^{-\frac{67000}{1.987 \cdot 1505}}\right);$

$1.860943710\ 10^{-10}$ (25)

$evalf\left(\frac{0.000001642931284}{1.860943710\ 10^{-10}}\right);$

8828.484576 (26)

Sample 9

$f := x \to 9 \cdot 10^{-11} \cdot e^{.0009 \cdot x};$

$$x \to \frac{9}{100000000000}\, e^{(0.0009x)} \tag{27}$$

$plot((f(x)),\ x = -10..141);$

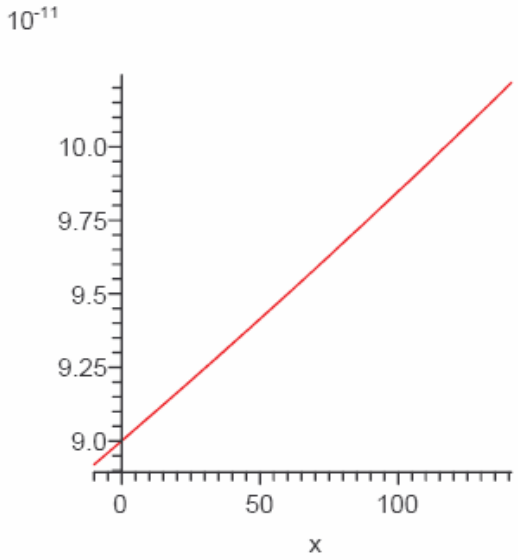

$evalf(int(f(x), x = 0..141));$

$$1.353034818\ 10^{-8} \tag{28}$$

$evalf\left(e^{-\frac{67000}{1.987 \cdot 1479}}\right);$

$$1.255106400\ 10^{-10} \tag{29}$$

$evalf\left(\frac{1.353034818\ 10^{-8}}{1.255106400\ 10^{-10}}\right);$

$$107.8023997 \tag{30}$$

Sample 10

$f := x \rightarrow .75 \cdot 10^{-13} \cdot x^2 - 5 \cdot 10^{-12} \cdot x + 2 \cdot 10^{-12};$

$$x \rightarrow \frac{0.75\,x^2}{10000000000000} - \frac{1}{200000000000}\,x + \frac{1}{500000000000} \tag{31}$$

$plot((f(x)),\ x = -10..145);$

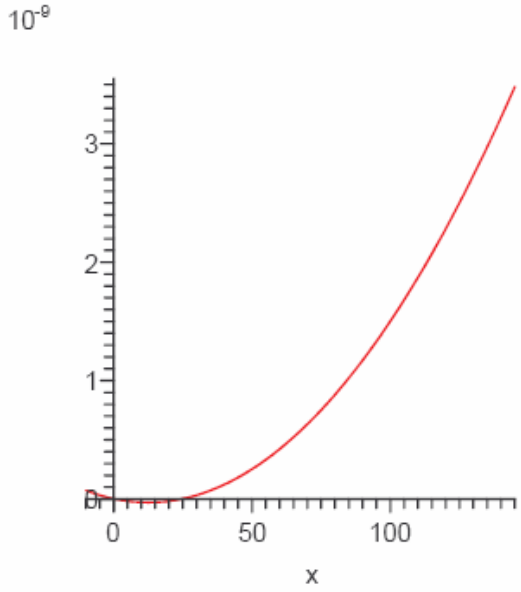

$evalf(int(f(x), x = 0..145));$

$$2.394312500\ 10^{-8} \tag{32}$$

$evalf\left(e^{-\frac{67000}{1.987 \cdot 1513}}\right);$

$$2.094990712\ 10^{-10} \tag{33}$$

$evalf\left(\frac{2.394312500\ 10^{-8}}{2.094990712\ 10^{-10}}\right);$

$$114.2874995 \tag{34}$$

Sample 11

$f := x \to 1 \cdot 10^{-10} \cdot e^{.00002 \cdot x};$

$$x \to \frac{1}{10000000000}\, e^{(0.00002\,x)} \tag{35}$$

$plot((f(x)),\ x = -10..141);$

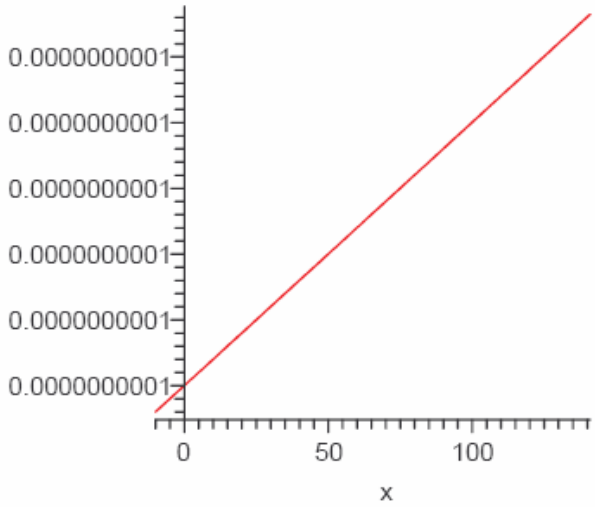

$evalf(int(f(x), x = 0..141));$

$$1.411989970\ 10^{-8} \tag{36}$$

$evalf\left(e^{-\frac{67000}{1.987 \cdot 1479}}\right);$

$$1.255106400\ 10^{-10} \tag{37}$$

$evalf\left(\frac{1.411989970\ 10^{-8}}{1.255106400\ 10^{-10}}\right);$

$$112.4996231 \tag{38}$$

Sample 12

$f := x \to 2 \cdot 10^{-10} \cdot e^{.00008 \cdot x};$

$$x \to \frac{1}{5000000000}\, e^{(0.00008\, x)} \tag{39}$$

$plot((f(x)),\ x = -10..145);$

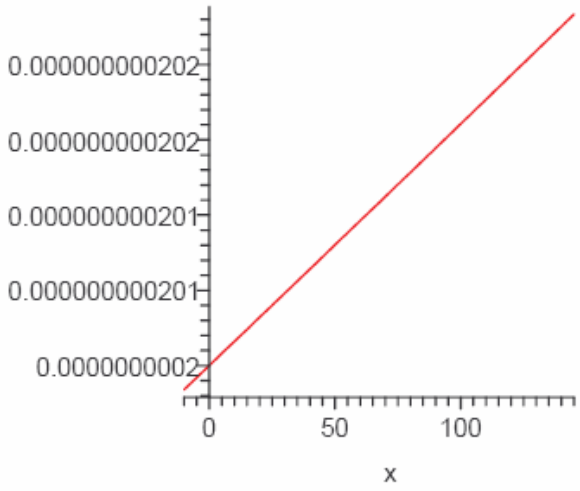

$evalf(int(f(x), x = 0..145));$

$$2.916885226\ 10^{-8} \tag{40}$$

$evalf\left(e^{-\frac{67000}{1.987 \cdot 1513}}\right);$

$$2.094990712\ 10^{-10} \tag{41}$$

$evalf\left(\frac{2.916885226\ 10^{-8}}{2.094990712\ 10^{-10}}\right);$

$$139.2314156 \tag{42}$$

Sample 13

$f := x \to 8 \cdot 10^{-15} \cdot e^{(0.0002 \cdot x)};$

$$x \to \frac{1}{125000000000000}\, e^{(0.0002\,x)} \tag{43}$$

$plot((f(x)),\ x = 0..52400);$

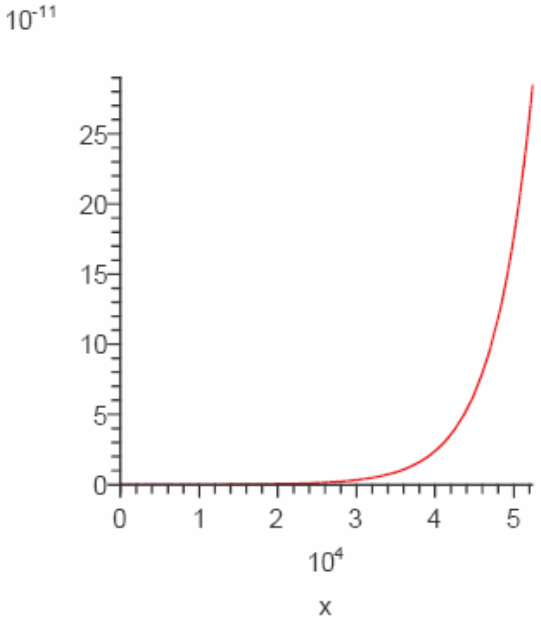

$evalf(int(f(x), x = 0..52400));$

$$0.000001423816302 \tag{44}$$

$evalf\left(e^{-\frac{67000}{1.987 \cdot 1479}}\right);$

$$1.255106400\ 10^{-10} \tag{45}$$

$evalf\left(\frac{0.000001423816302}{1.255106400\ 10^{-10}}\right);$

$$11344.18805 \tag{46}$$

Sample 14

$f := x \to 2 \cdot 10^{-12} \cdot e^{0.0001 \cdot x};$

$$x \to \frac{1}{500000000000} e^{(0.0001 x)} \tag{47}$$

$plot((f(x)),\ x = -10..60200);$

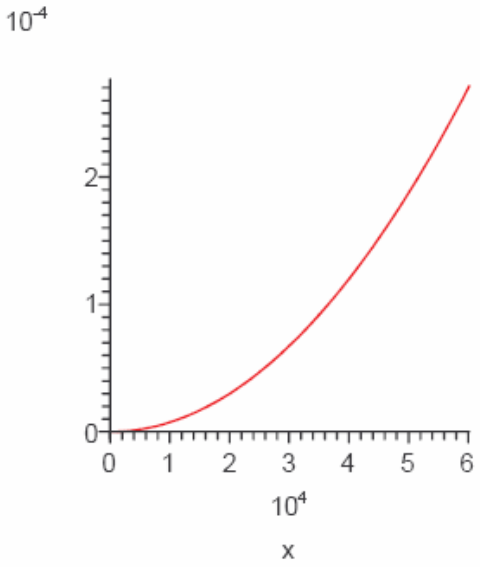

$evalf(int(f(x), x = 0..50200));$

$$0.000003008226076 \tag{48}$$

$evalf\left(e^{-\frac{67000}{1.987 \cdot 1513}}\right);$

$$2.094990712\ 10^{-10} \tag{49}$$

$$evalf\left(\frac{0.000003008226076}{2.094990712\ 10^{-10}}\right);$$

$$14359.13801 \tag{50}$$

Sample 15

$$f := x \to 8 \cdot 10^{-15} \cdot e^{(0.0002 \cdot x)}$$

$$x \to \frac{1}{125000000000000}\ e^{(0.0002x)} \tag{51}$$

$$plot((f(x)),\ x = -10..58100);$$

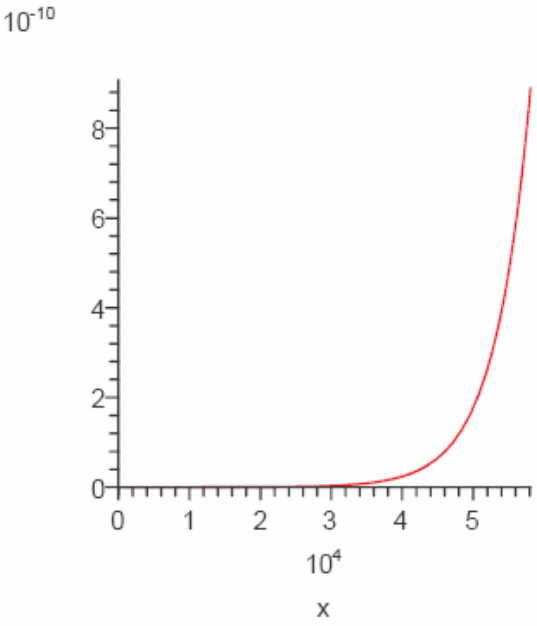

$$evalf(int(f(x), x = 0..52000));$$

$$0.000001314345027 \tag{52}$$

$$evalf\left(e^{-\frac{67000}{1.987 \cdot 1479}}\right);$$

$$1.255106400\ 10^{-10} \tag{53}$$

$$evalf\left(\frac{0.000001314345027}{1.255106400\ 10^{-10}}\right);$$

$$10471.98092 \tag{54}$$

Sample 16

$$f := x \to 2\cdot 10^{-12}\cdot e^{0.0001\cdot x}$$

$$x \to \frac{1}{500000000000}\, e^{(0.0001x)} \tag{55}$$

$$plot((f(x)),\ x = -10..58100);$$

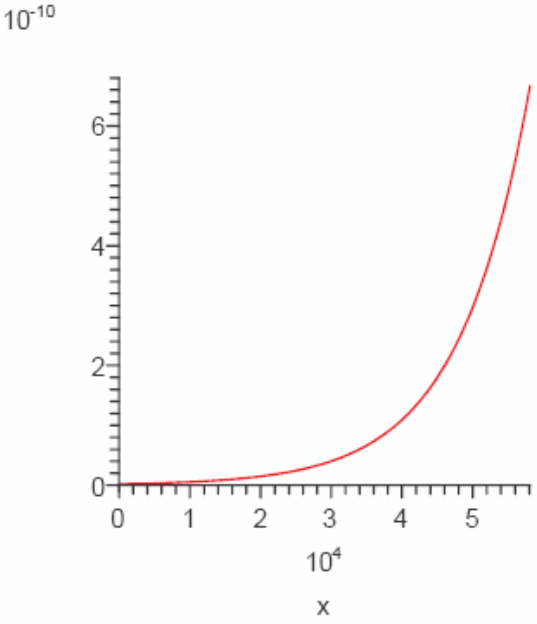

$$evalf(int(f(x), x = 0..52000));$$

$$0.000003605444838 \tag{56}$$

$$evalf\left(e^{-\frac{67000}{1.987\cdot 1513}}\right);$$

$$2.094990712\ 10^{-10} \tag{57}$$

$$evalf\left(\frac{0.000003605444838}{2.094990712\ 10^{-10}}\right); \qquad 17209.83686 \tag{58}$$

8.2 Appendix B: Grain Diameter Versus Effective Time Graphs

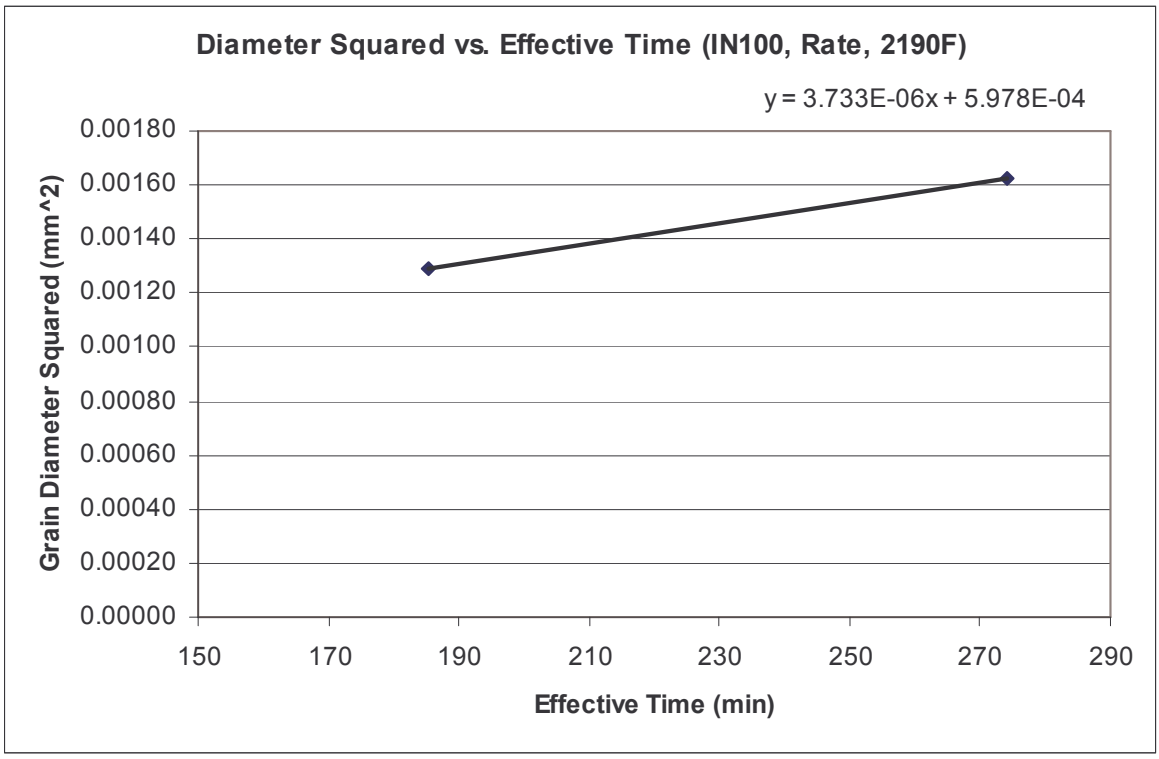

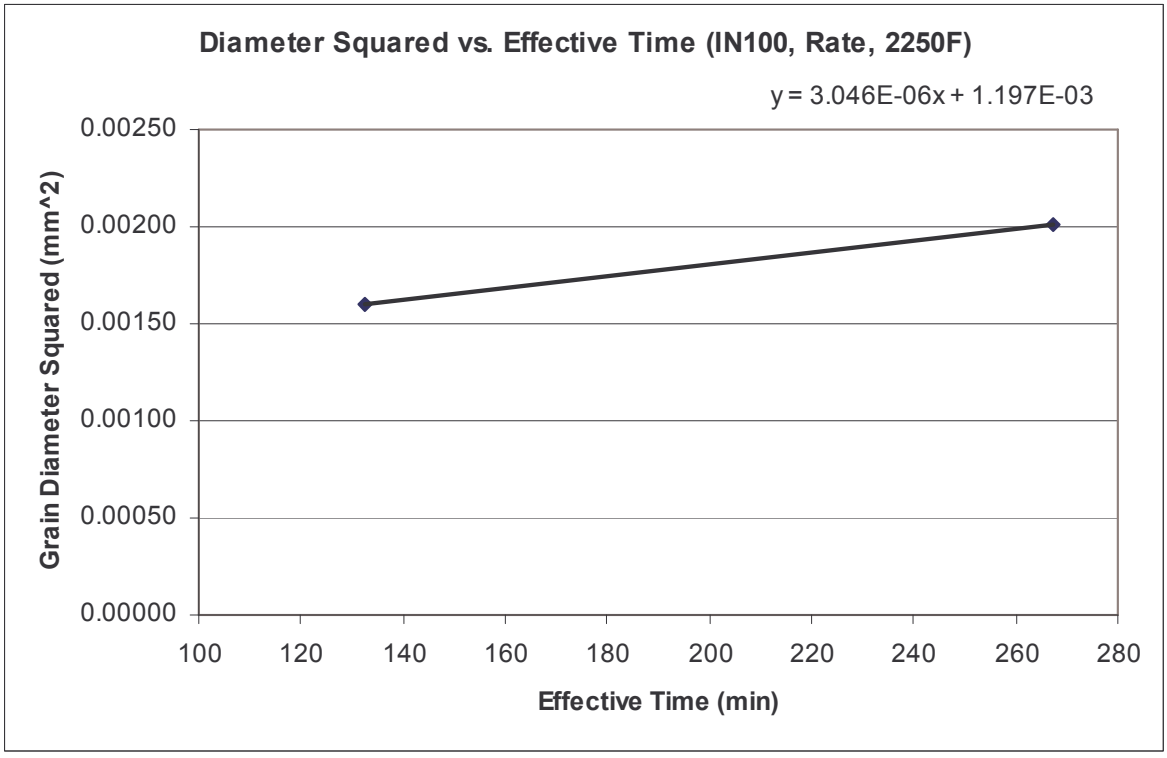

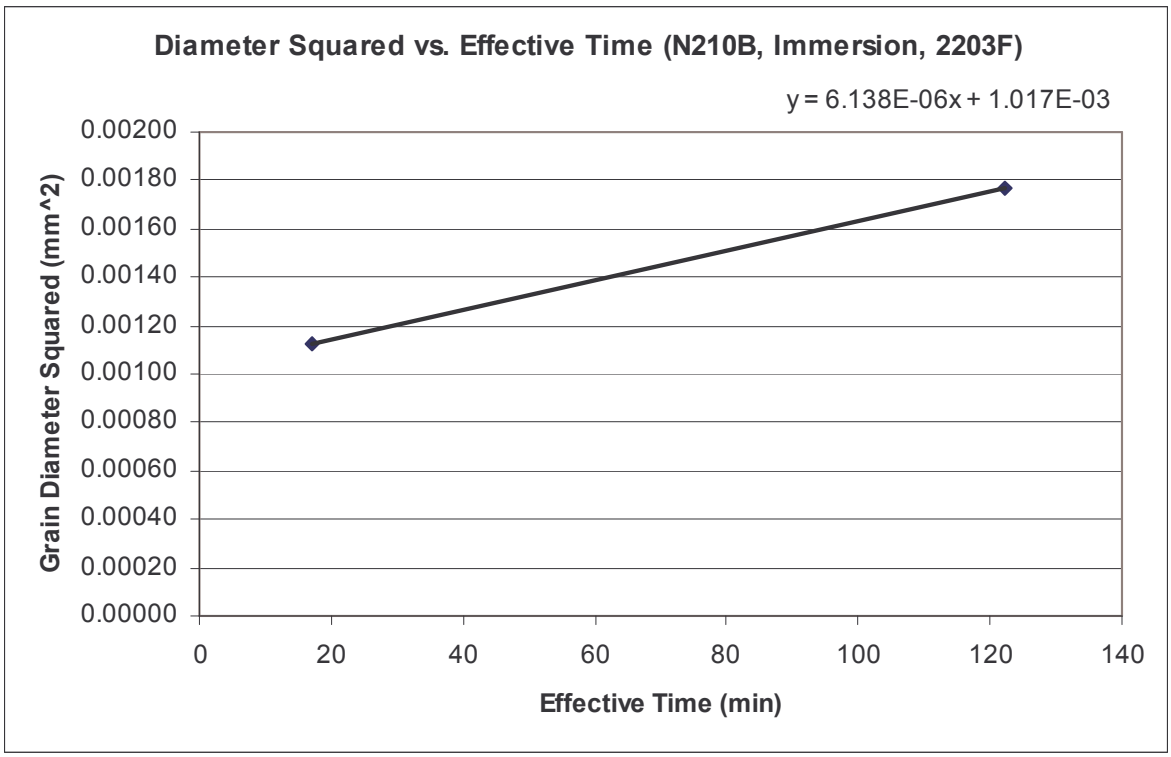
Diameter Squared vs. Effective Time (N210B, Immersion, 2203F)
y = 6.138E-06x + 1.017E-03
Grain Diameter Squared (mm^2)
0.00200
0.00180
0.00160
0.00140
0.00120
0.00100
0.00080
0.00060
0.00040
0.00020
0.00000
0
20
40
60
80
100
120
140
Effective Time (min)

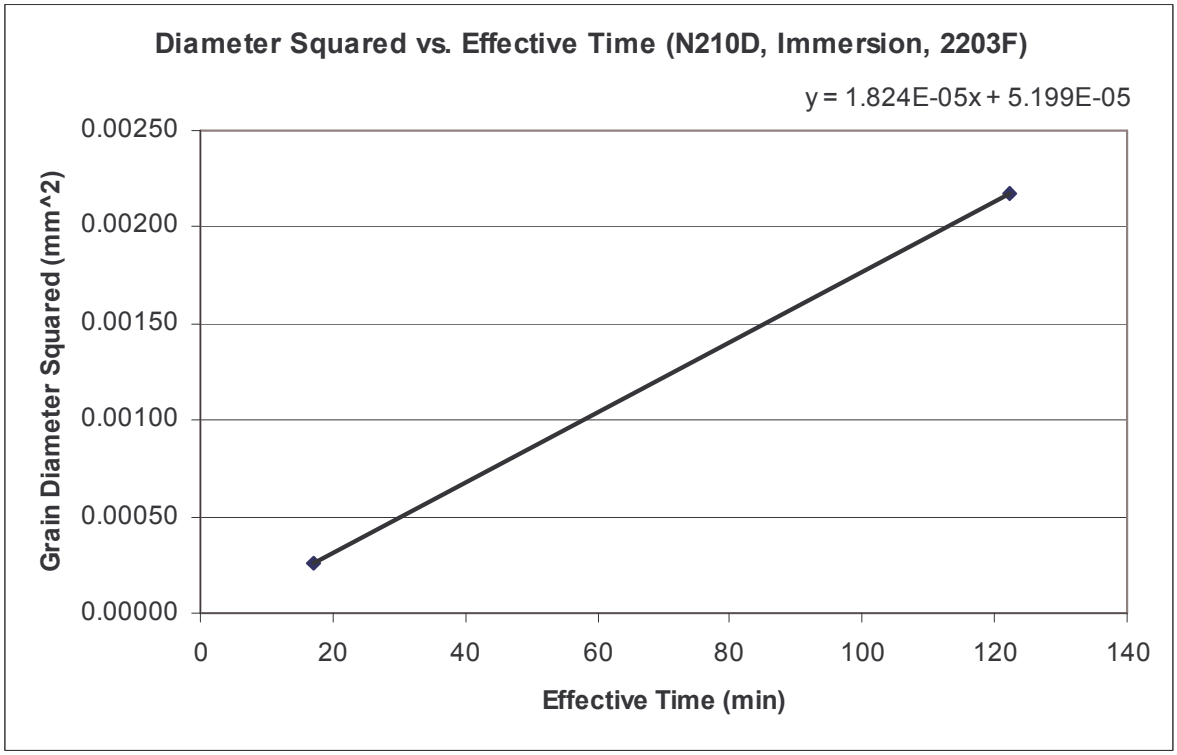
Diameter Squared vs. Effective Time (N210D, Immersion, 2203F)
y = 1.824E-05x + 5.199E-05
Grain Diameter Squared (mm^2)
0.00250
0.00200
0.00150
0.00100
0.00050
0.00000
0
20
40
60
80
100
120
140
Effective Time (min)

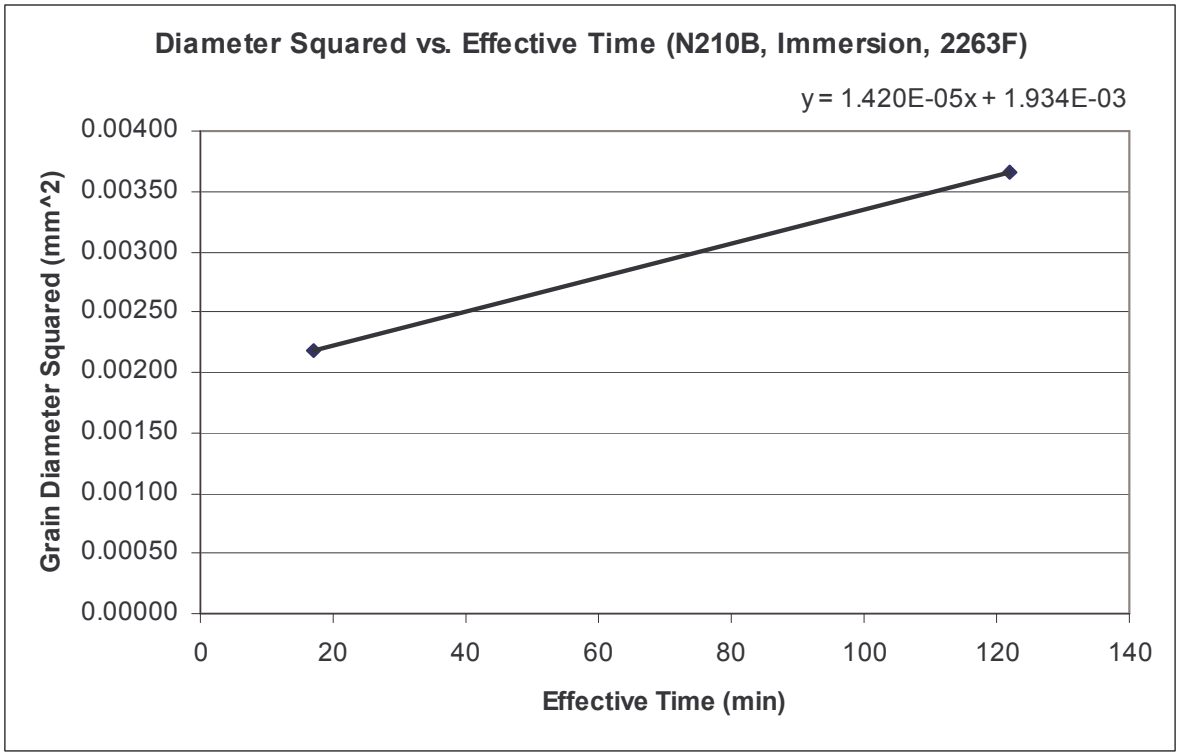
Diameter Squared vs. Effective Time (N210B, Immersion, 2263F)
y = 1.420E-05x + 1.934E-03
Grain Diameter Squared (mm^2)
0.00400
0.00350
0.00300
0.00250
0.00200
0.00150
0.00100
0.00050
0.00000
0
20
40
60
80
100
120
140
Effective Time (min)

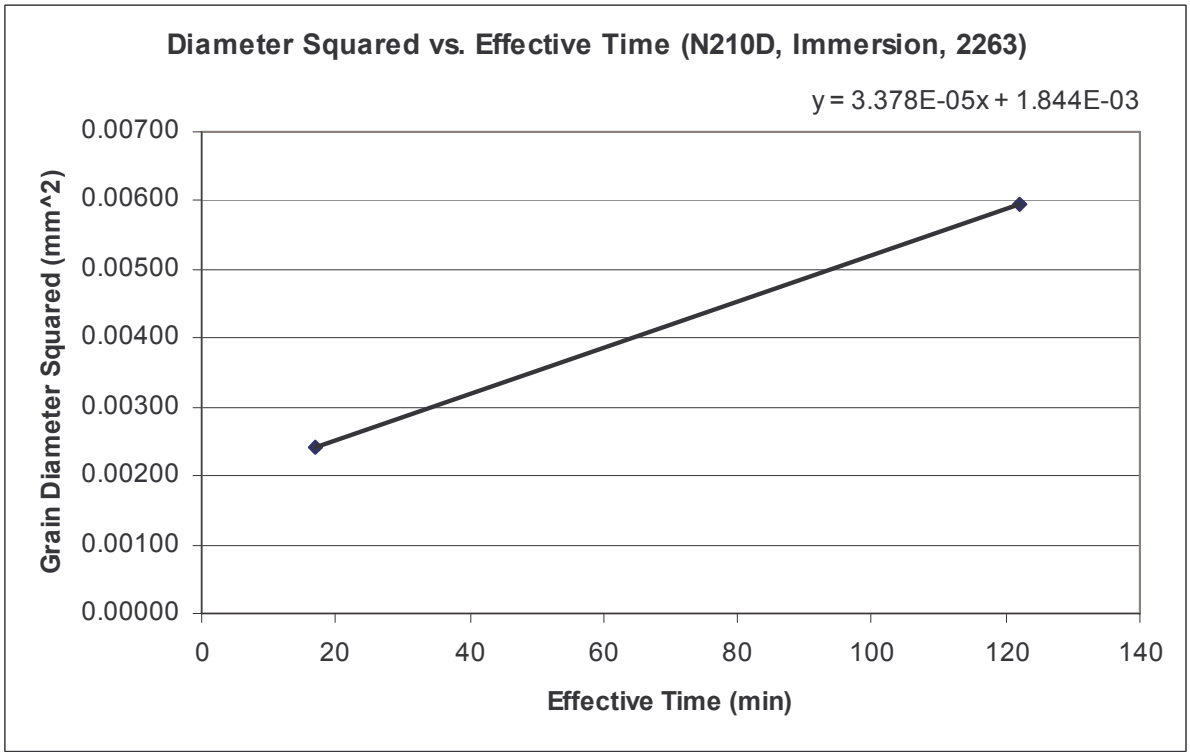
Diameter Squared vs. Effective Time (N210D, Immersion, 2263)
y = 3.378E-05x + 1.844E-03
Grain Diameter Squared (mm^2)
0.00700
0.00600
0.00500
0.00400
0.00300
0.00200
0.00100
0.00000
0
20
40
60
80
100
120
140
Effective Time (min)

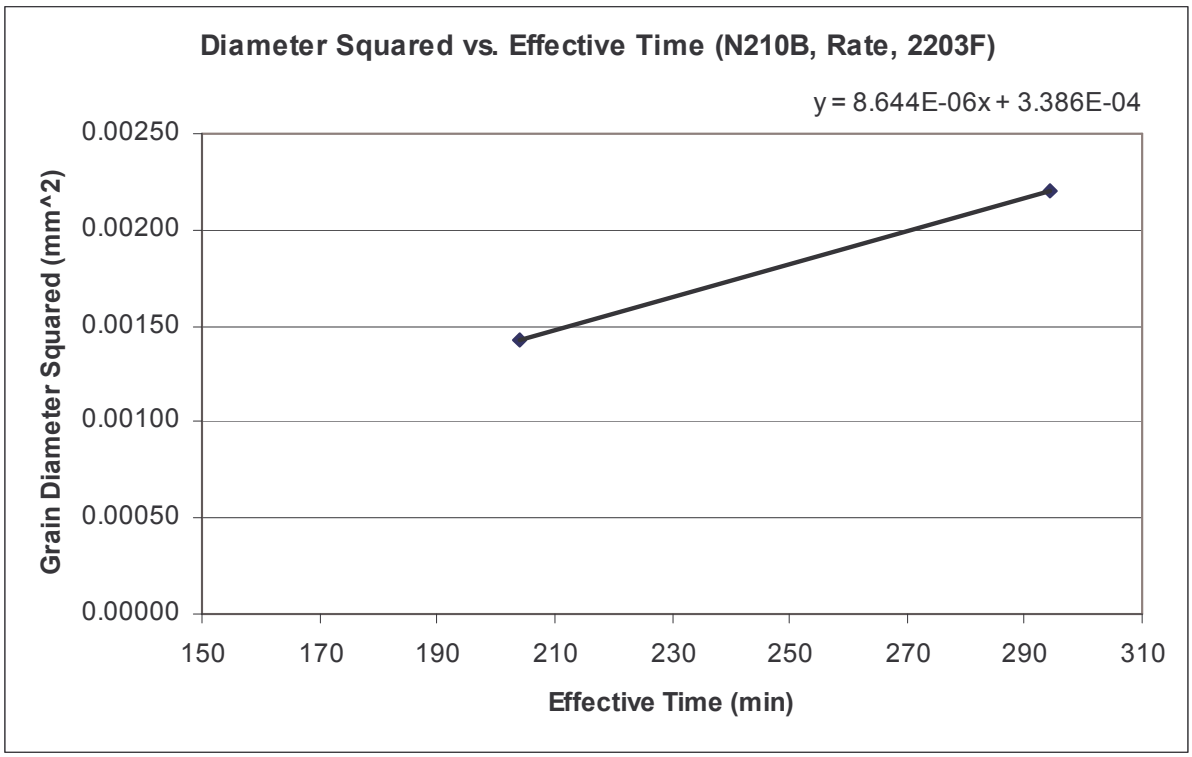
Diameter Squared vs. Effective Time (N210B, Rate, 2203F)
y = 8.644E-06x + 3.386E-04
Grain Diameter Squared (mm^2)
0.00250
0.00200
0.00150
0.00100
0.00050
0.00000
150
170
190
210
230
250
270
290
310
Effective Time (min)

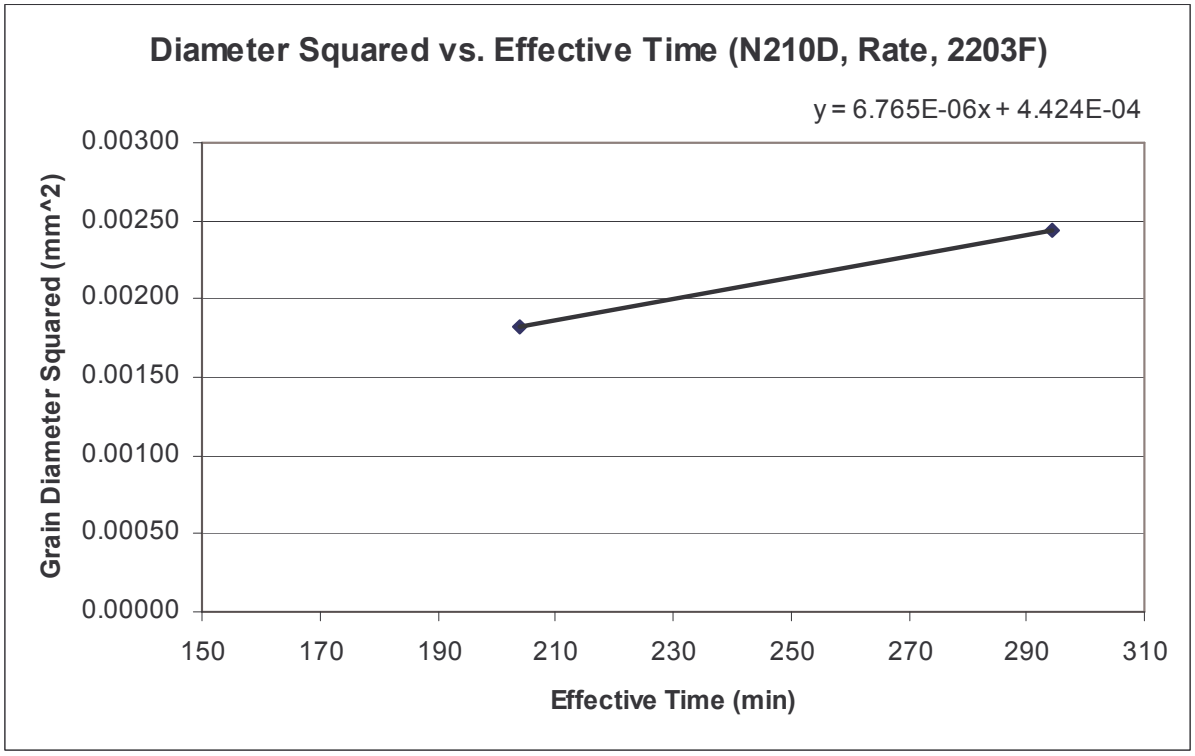
Diameter Squared vs. Effective Time (N210D, Rate, 2203F)
y = 6.765E-06x + 4.424E-04
Grain Diameter Squared (mm^2)
0.00300
0.00250
0.00200
0.00150
0.00100
0.00050
0.00000
150
170
190
210
230
250
270
290
310
Effective Time (min)

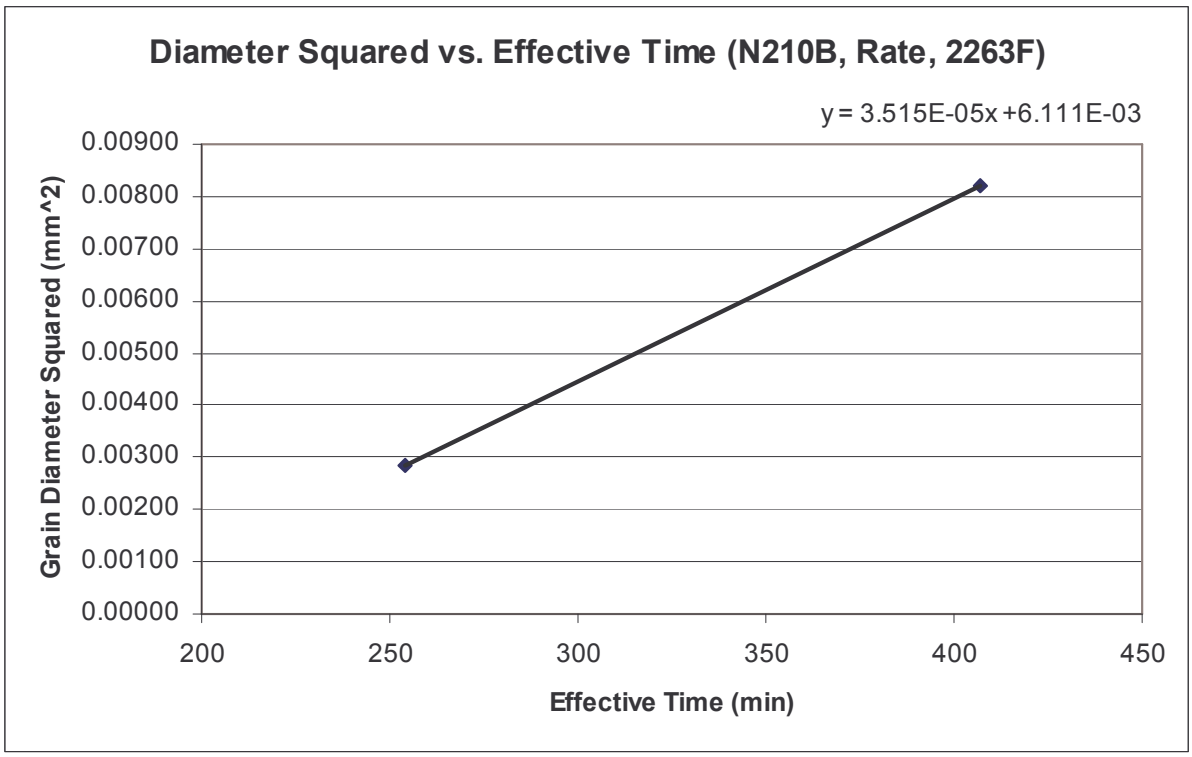
Diameter Squared vs. Effective Time (N210B, Rate, 2263F)
y = 3.515E-05x +6.111E-03
Grain Diameter Squared (mm^2)
0.00900
0.00800
0.00700
0.00600
0.00500
0.00400
0.00300
0.00200
0.00100
0.00000
200
250
300
350
400
450
Effective Time (min)

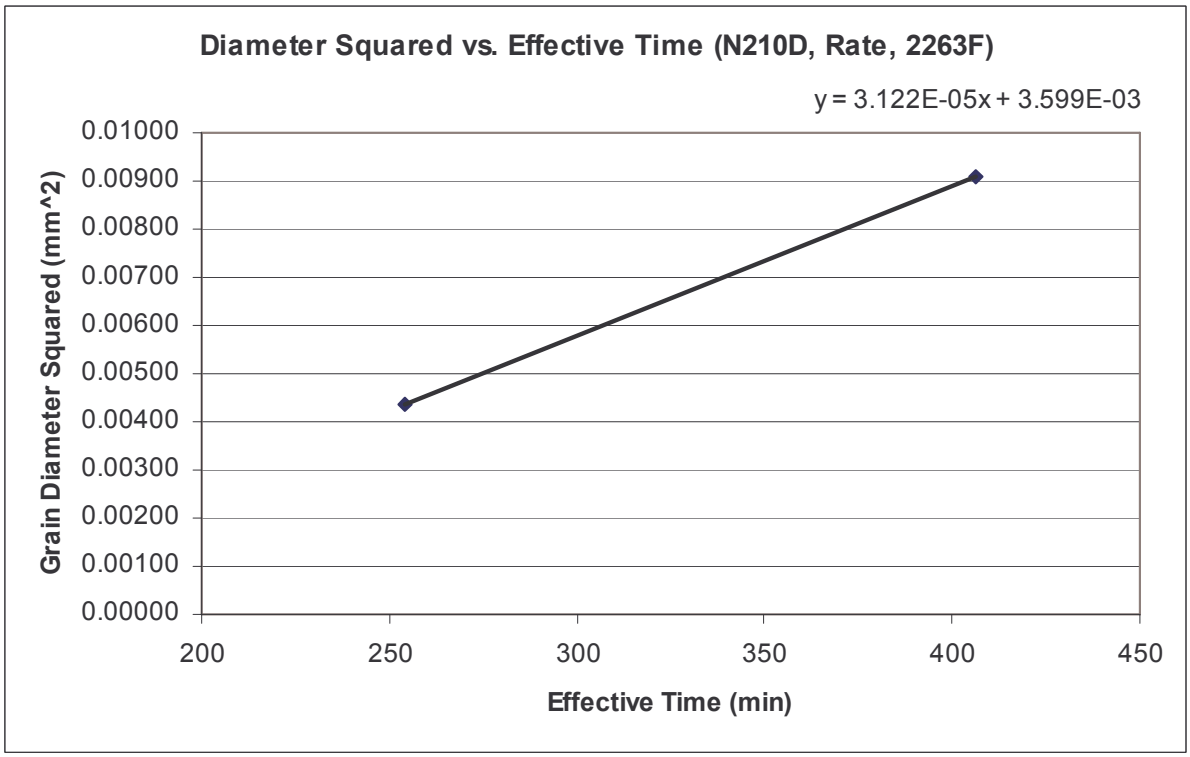
Diameter Squared vs. Effective Time (N210D, Rate, 2263F)
y = 3.122E-05x + 3.599E-03
Grain Diameter Squared (mm^2)
0.01000
0.00900
0.00800
0.00700
0.00600
0.00500
0.00400
0.00300
0.00200
0.00100
0.00000
200
250
300
350
400
450
Effective Time (min)

8.3 Appendix C: Specimen Pictures

Sample 1:

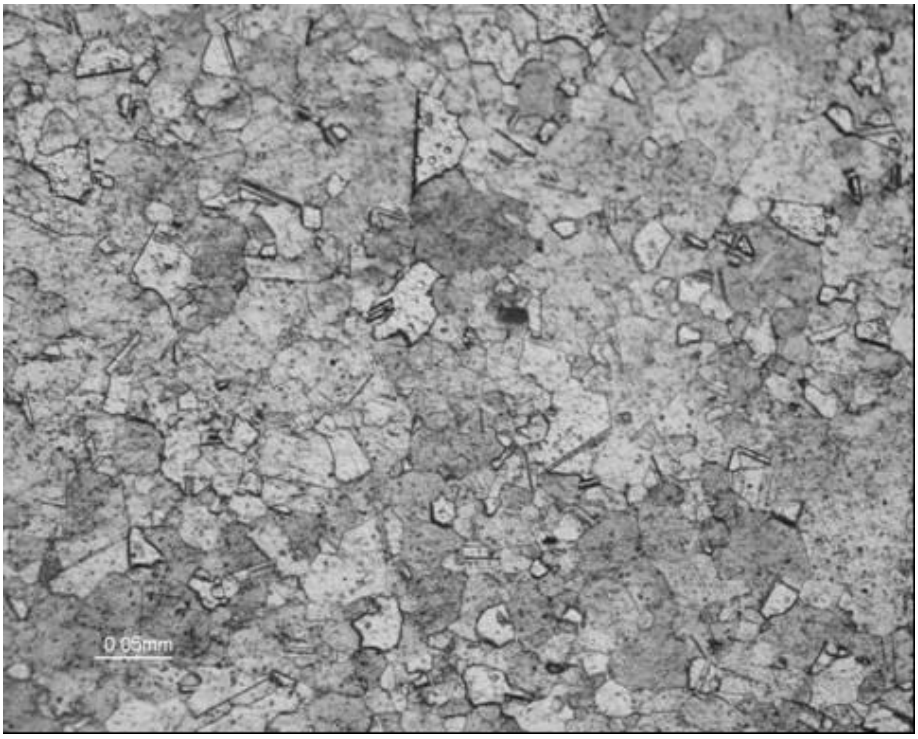

Sample 2:

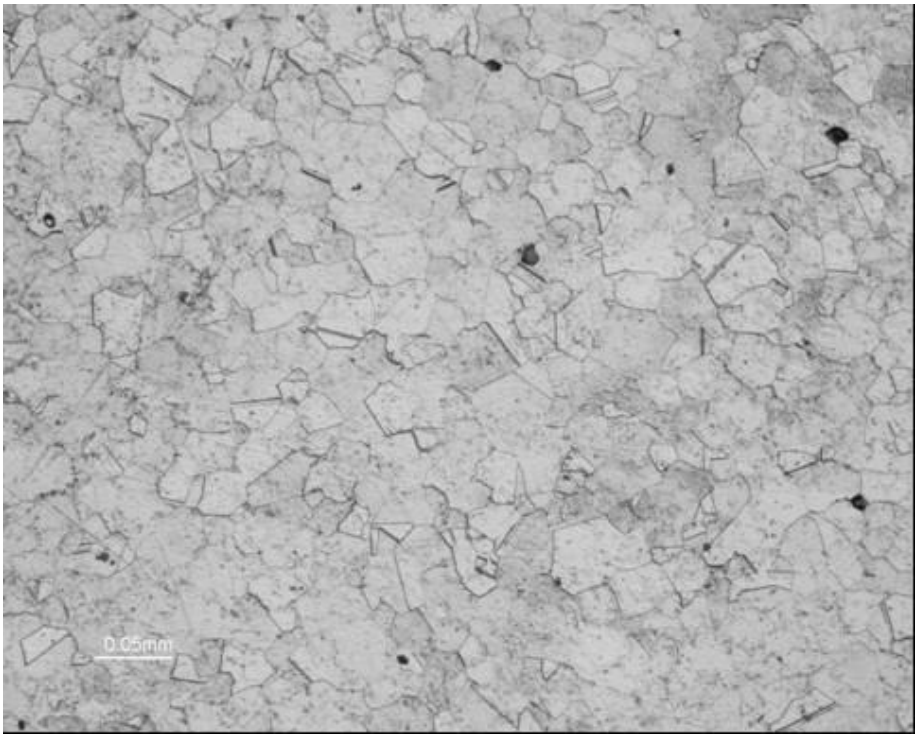

Sample 3:

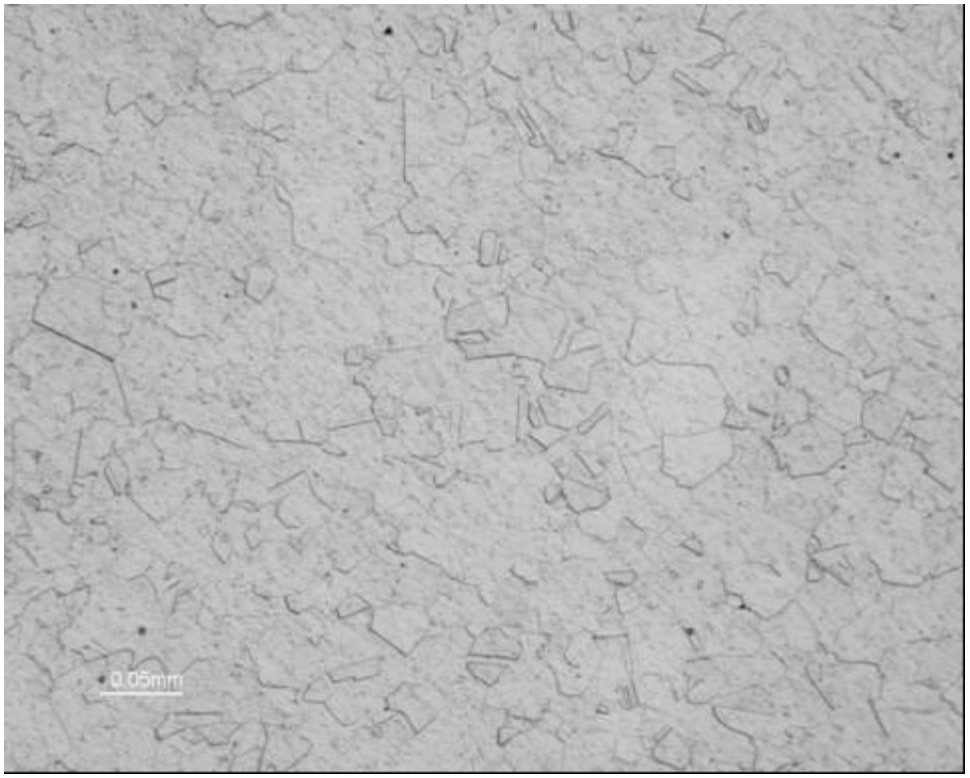

Sample 4:

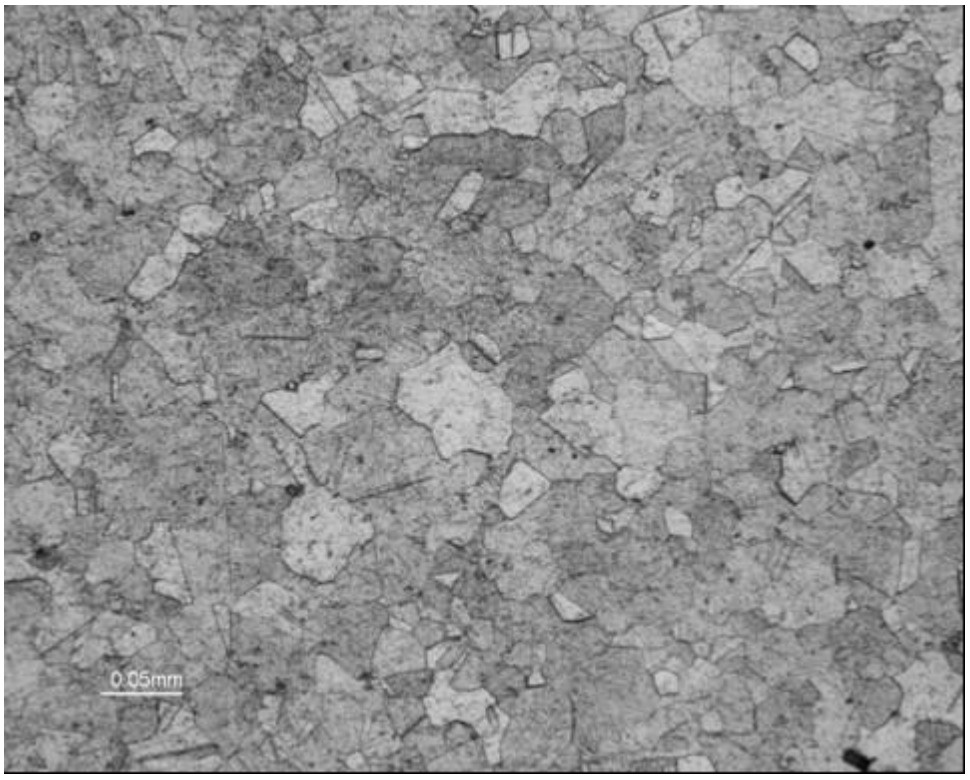

Sample 5:

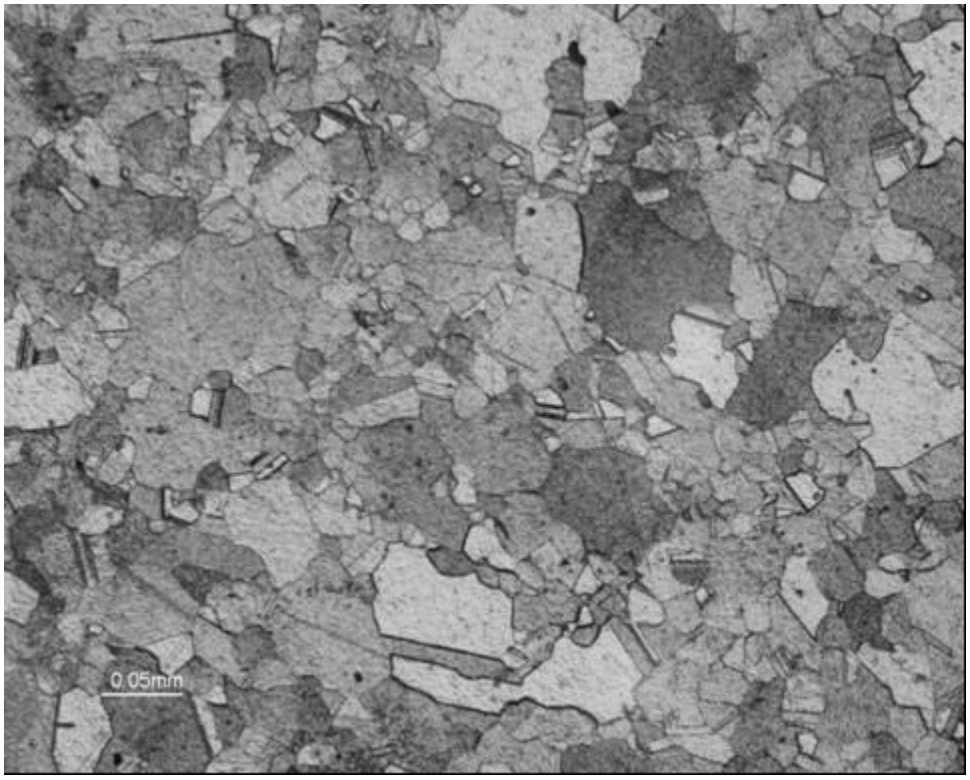

Sample 6:

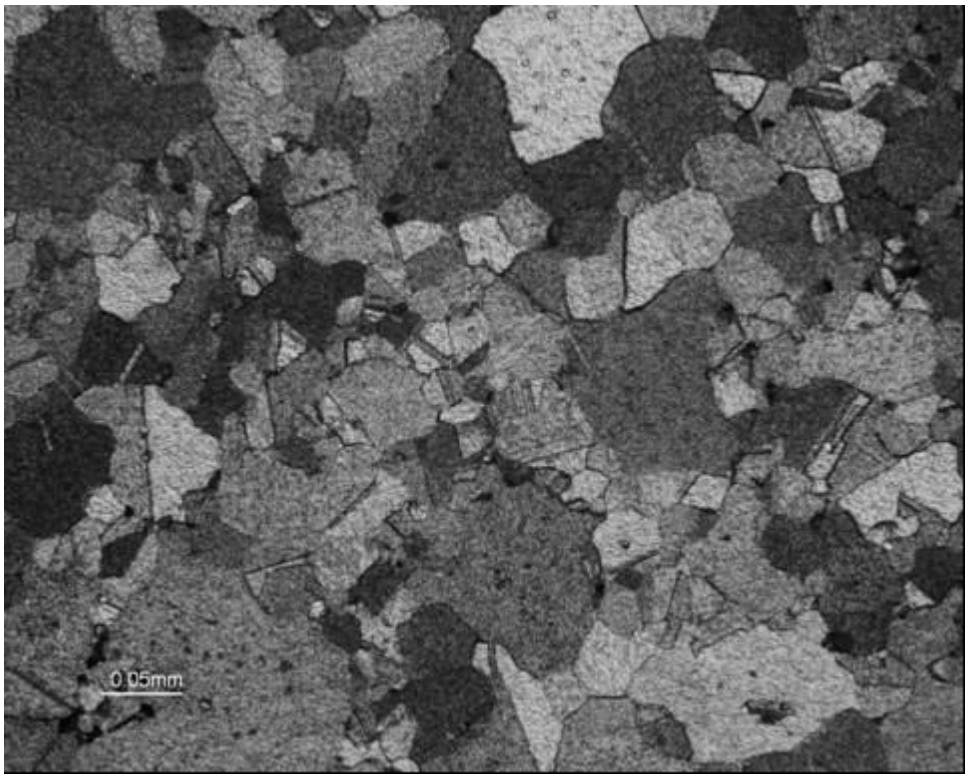

Sample 7:

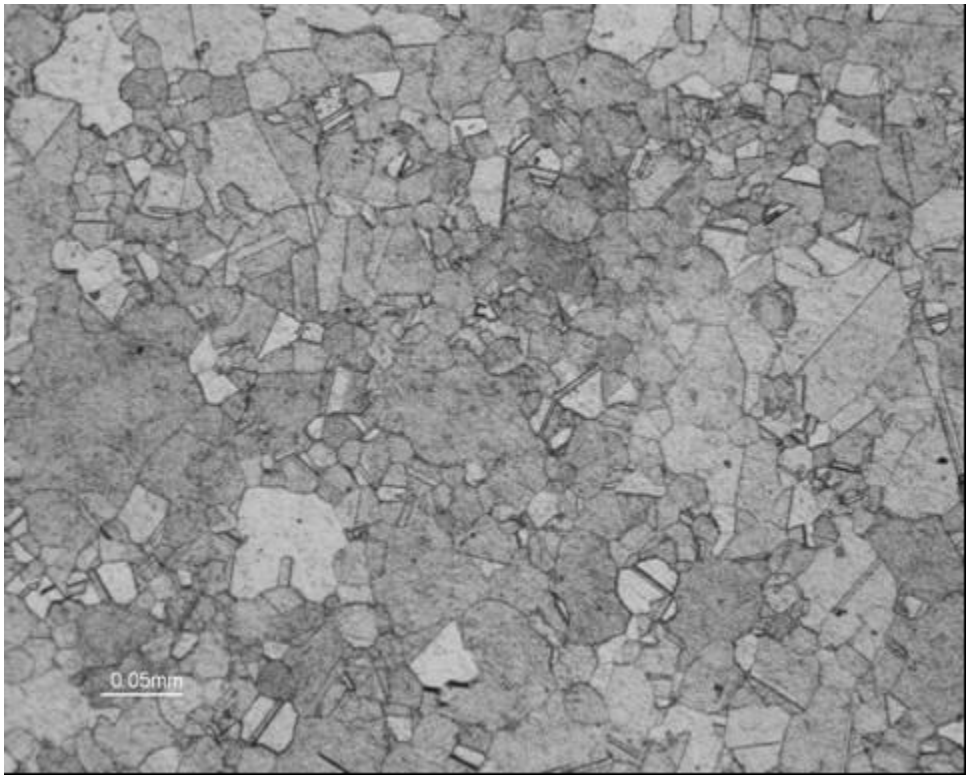

Sample 8:

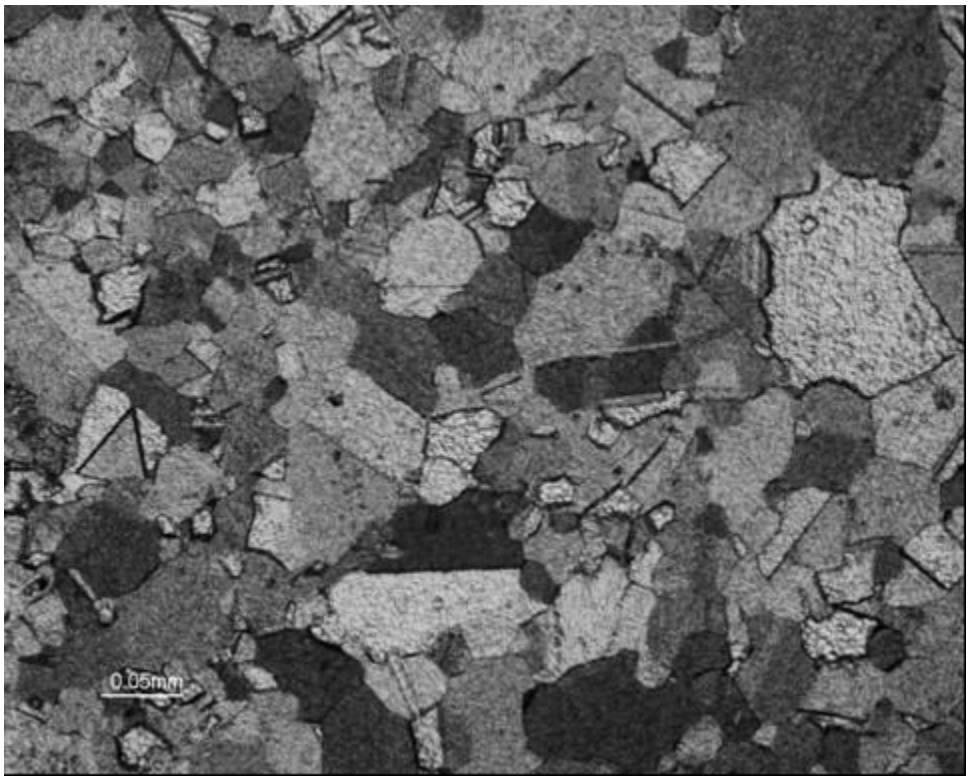

Sample 9b:

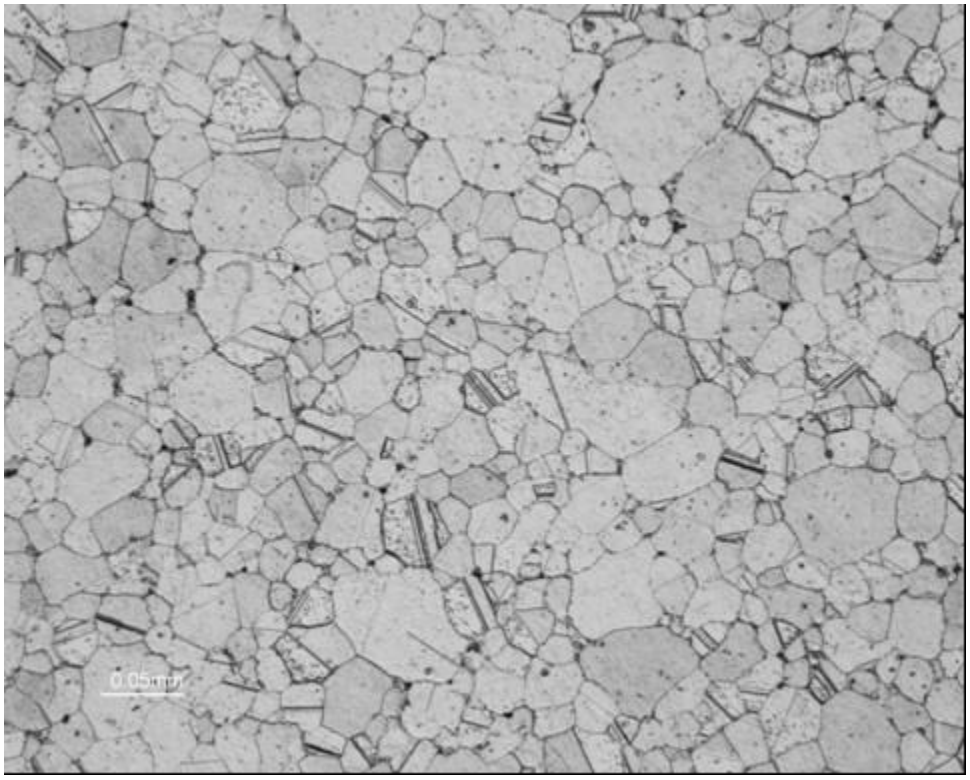

Sample 9d:

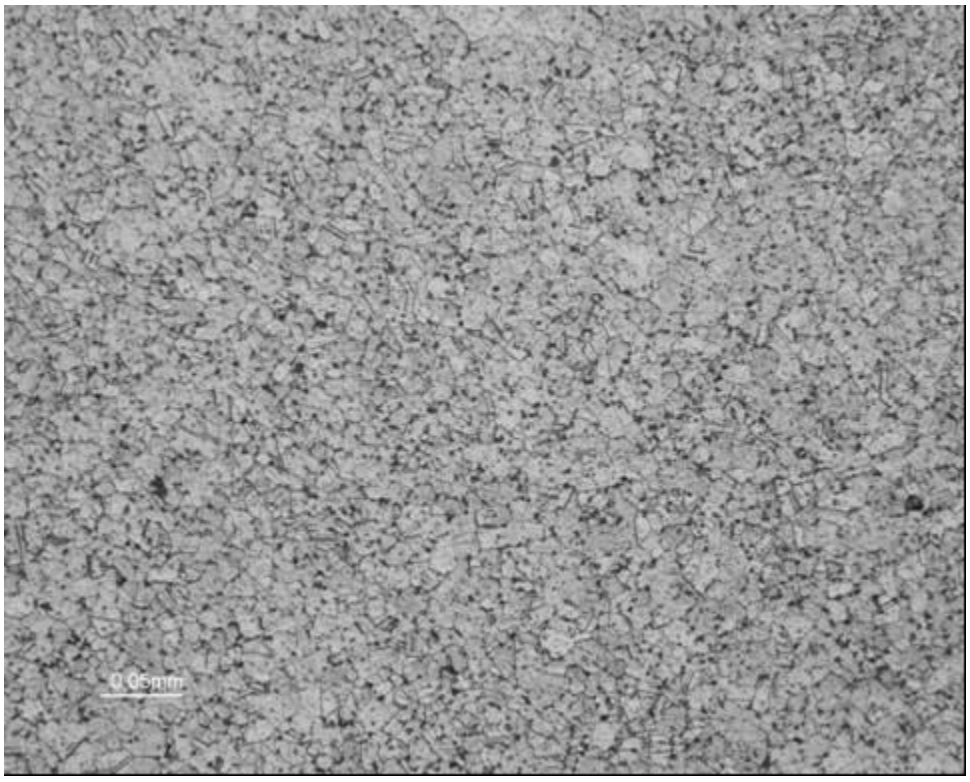

Sample 10b:

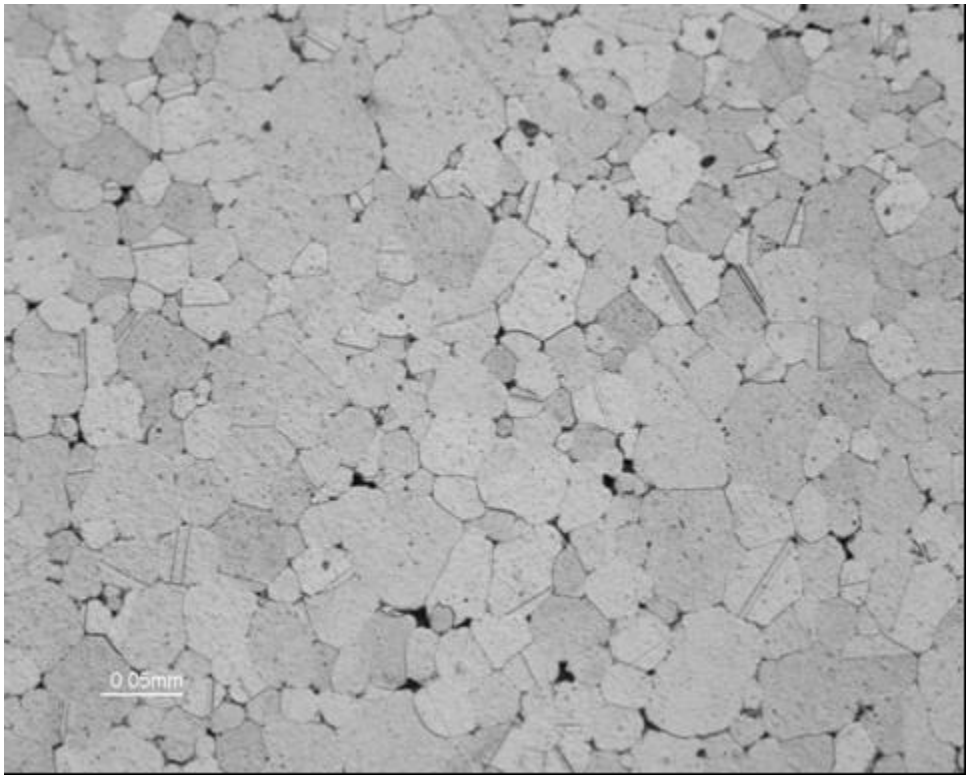

Sample 10d:

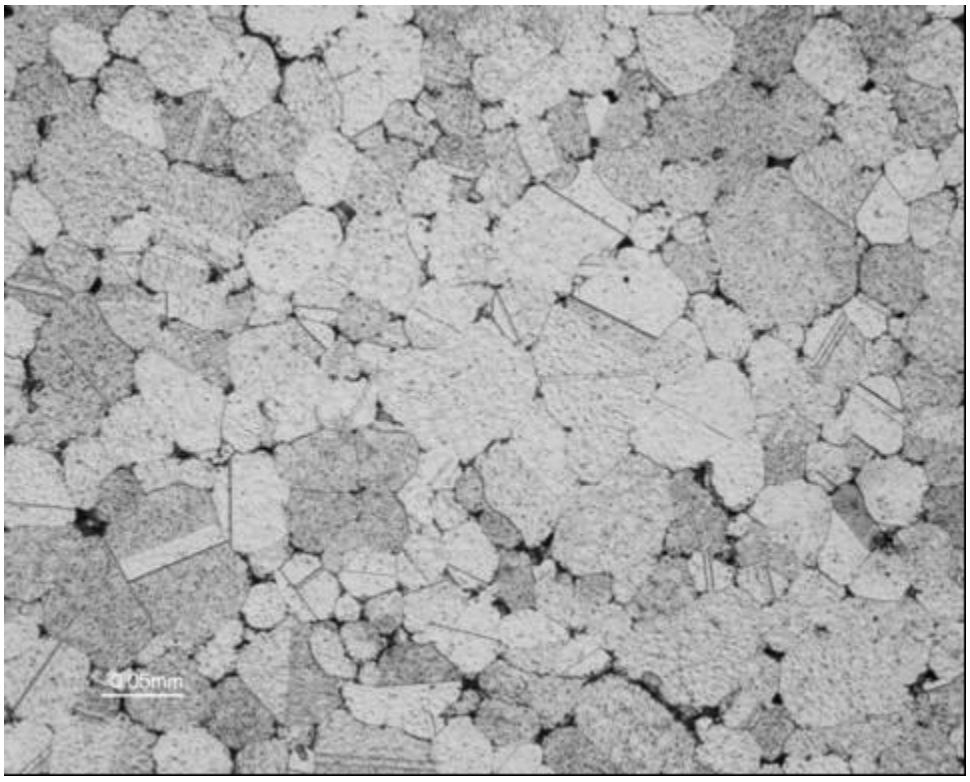

Sample 11b:

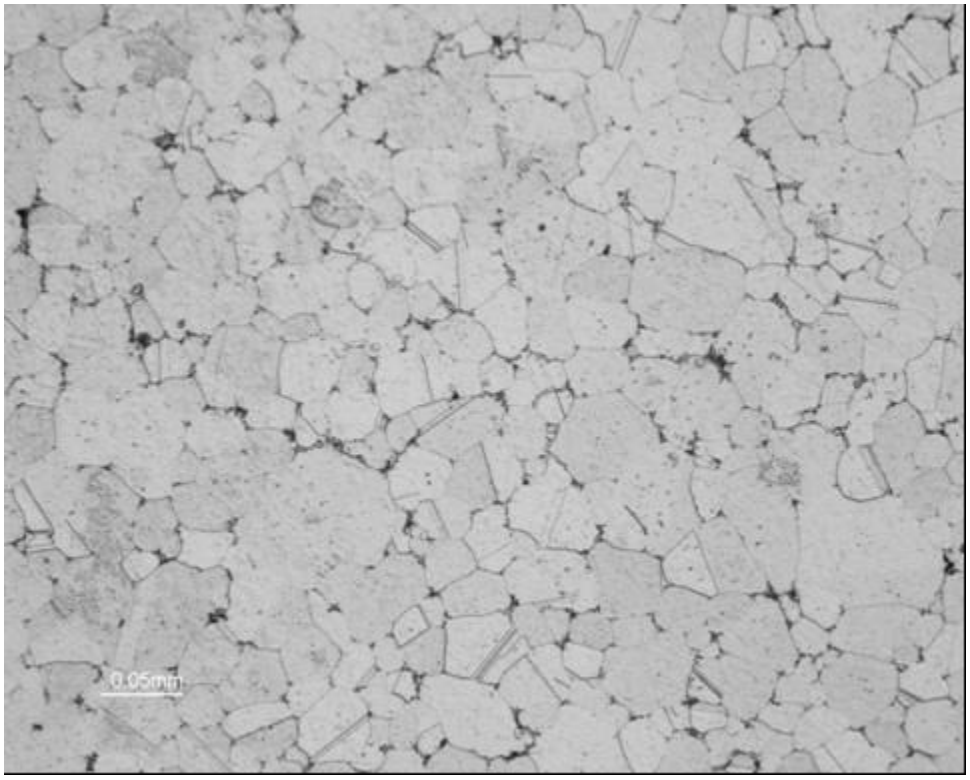

Sample 11d:

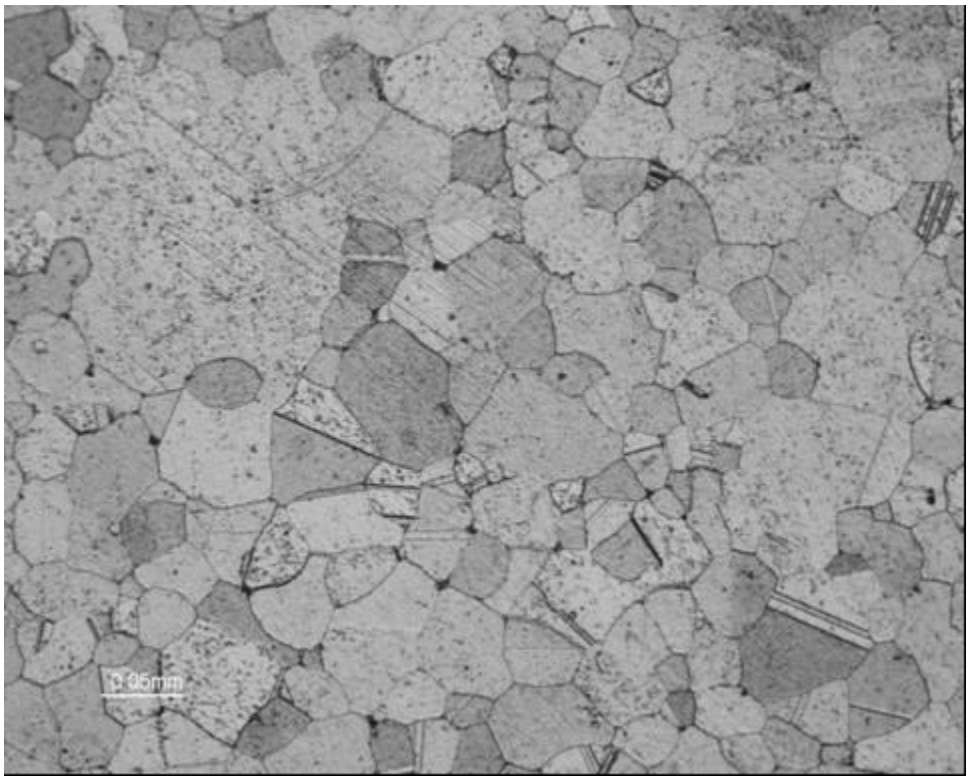

Sample 12b:

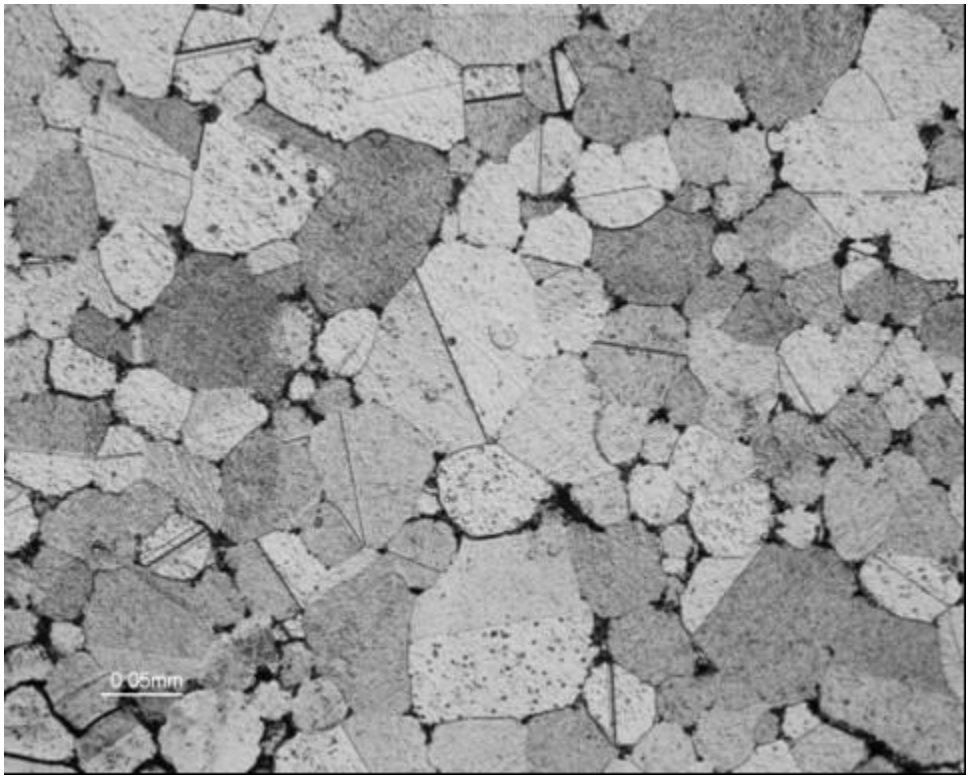

Sample 12d:

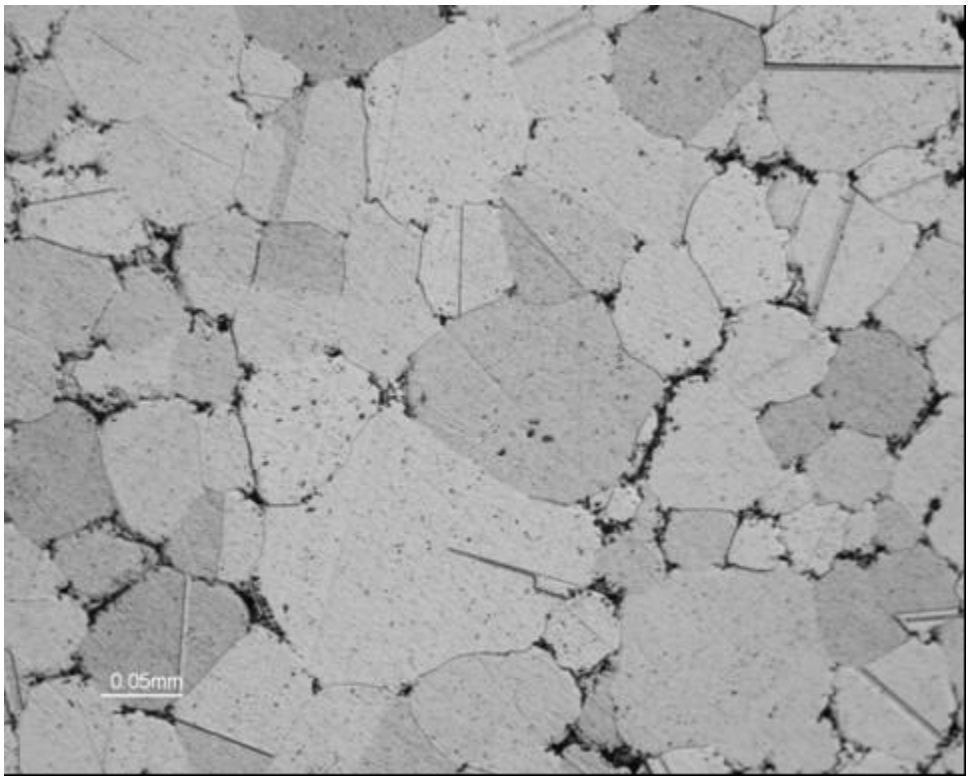

Sample 13b:

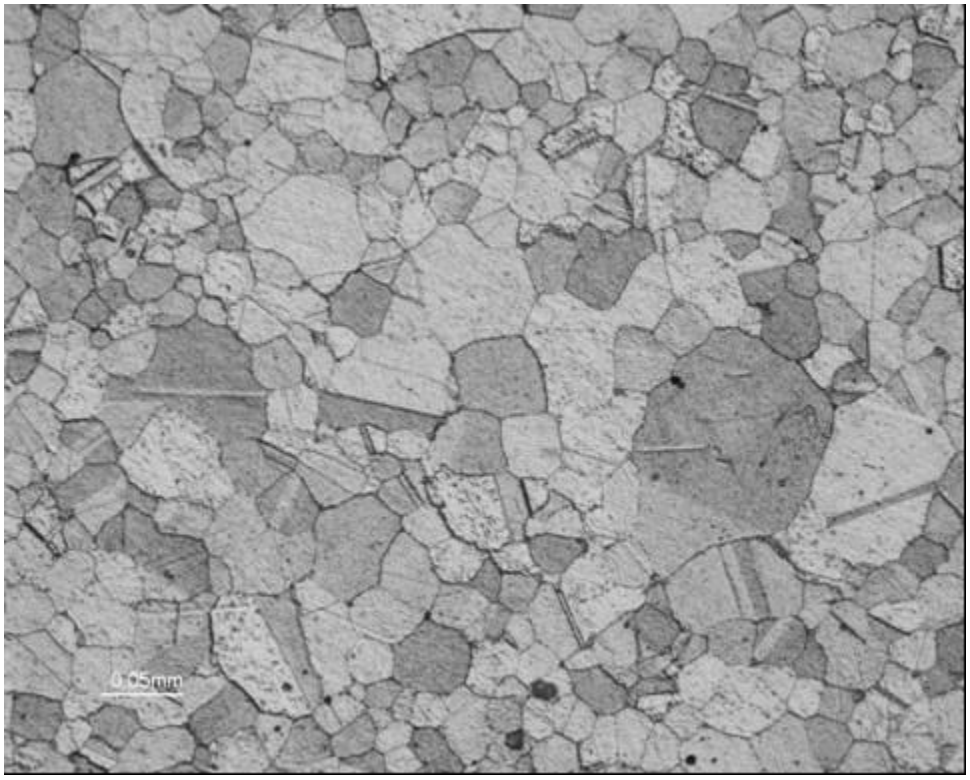

Sample 13d:

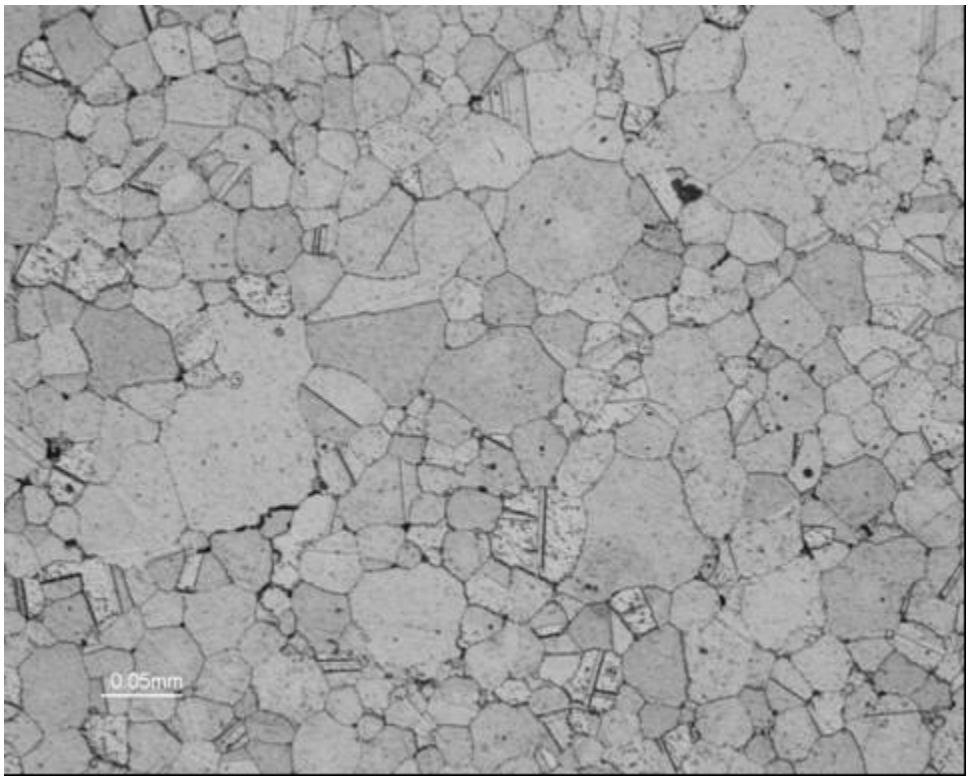

Sample 14b:

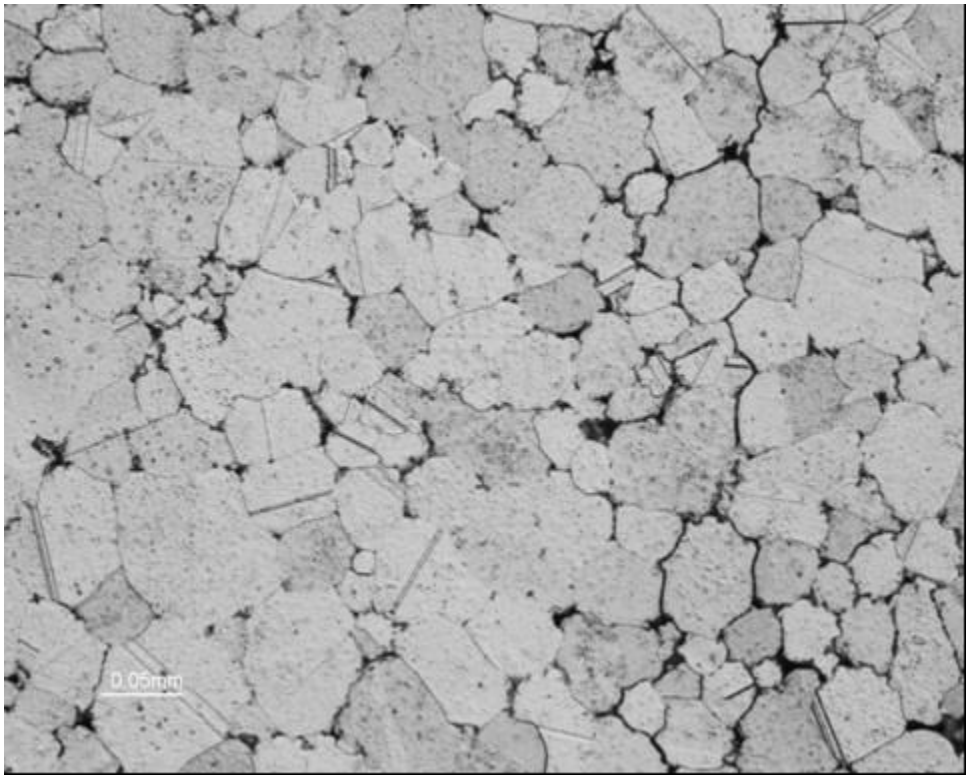

Sample 14d:

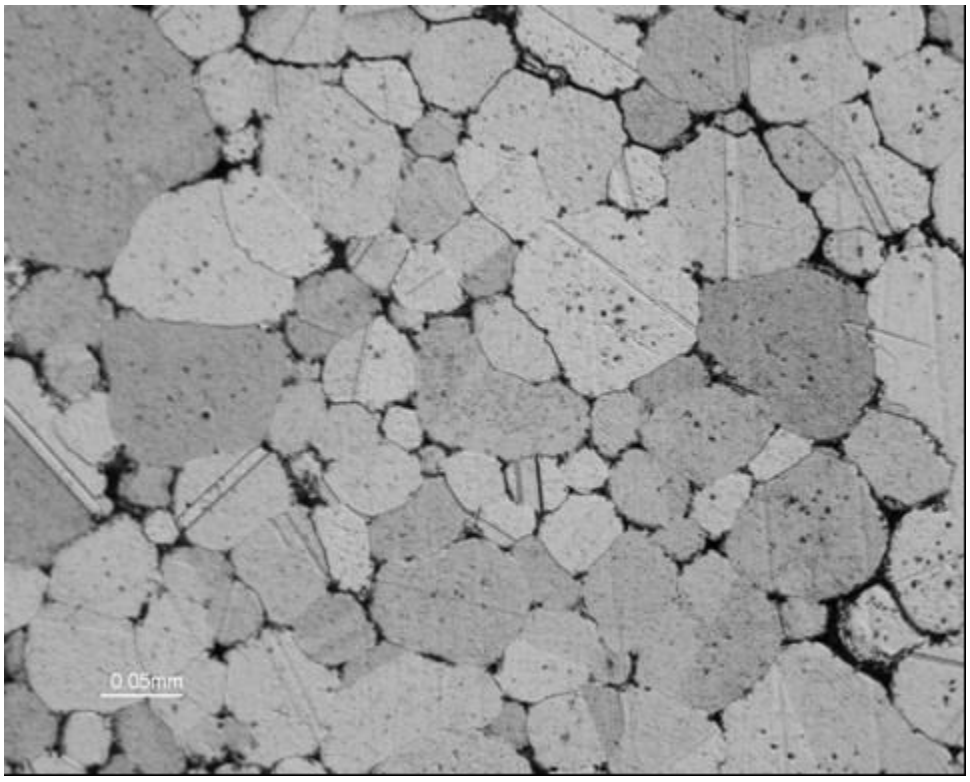

Sample 15b:

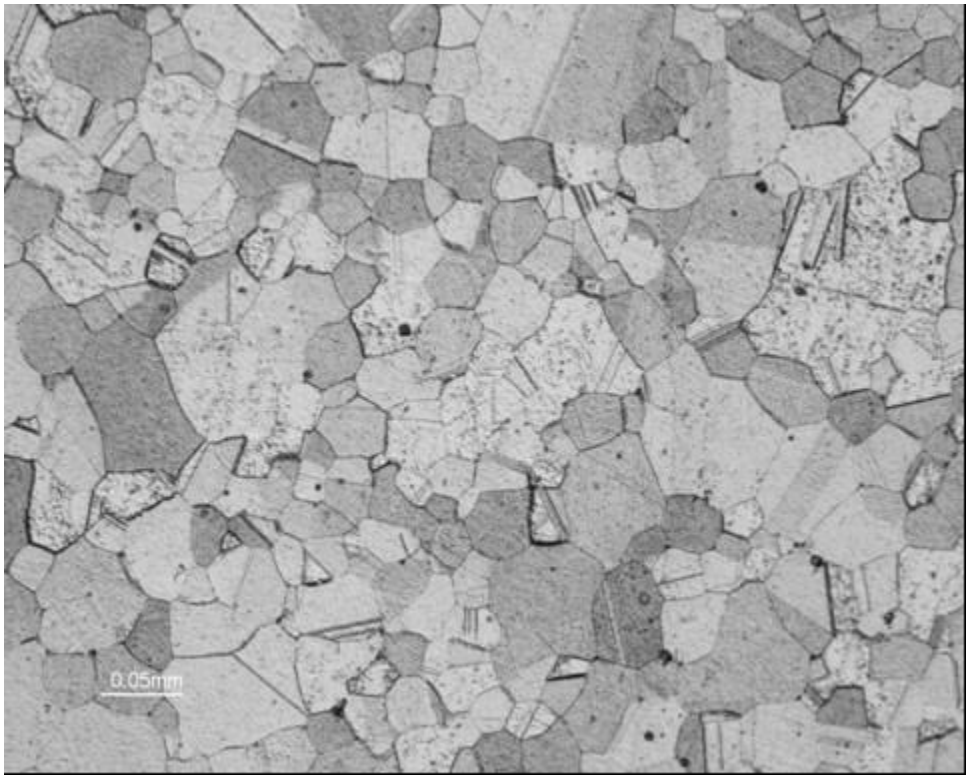

Sample 15d:

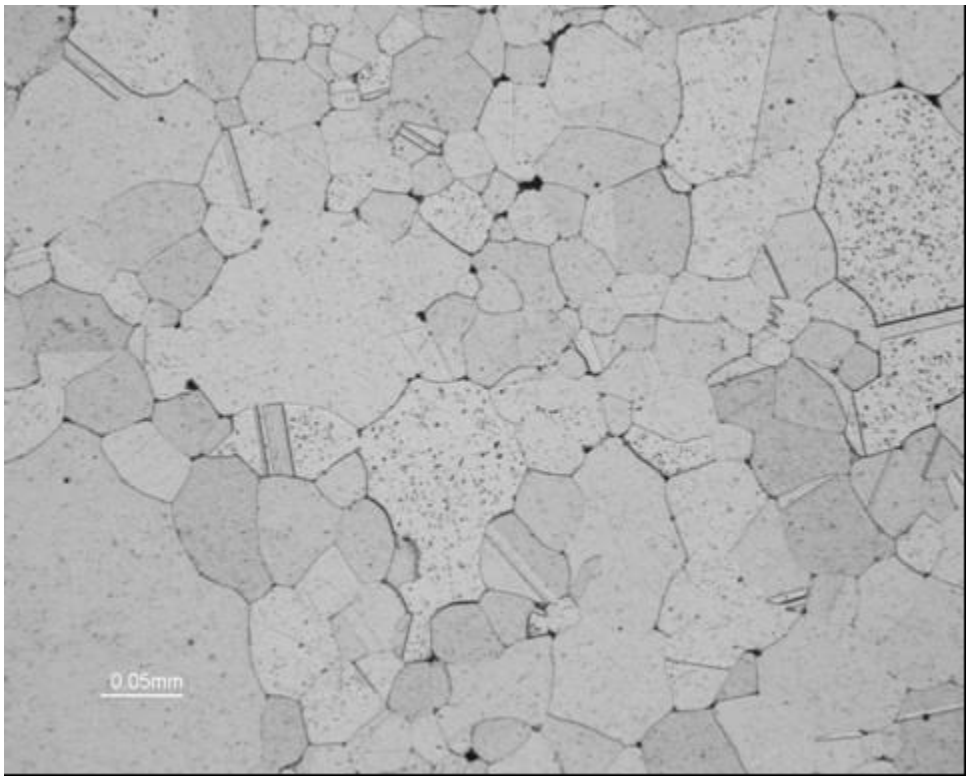

Sample 16b:

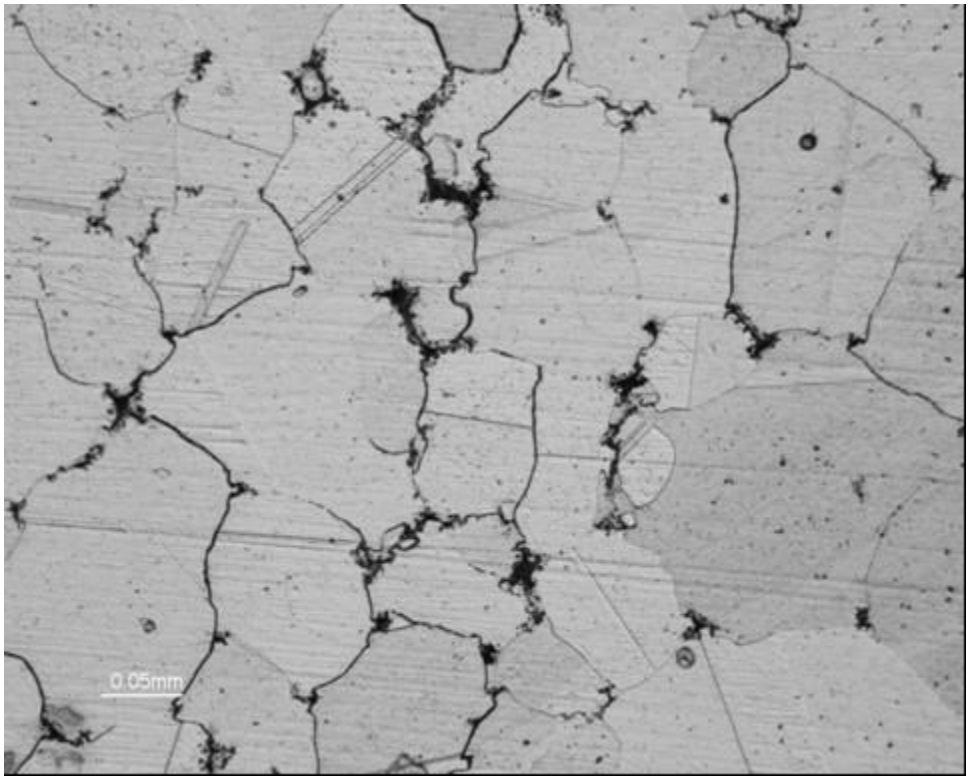

Sample 16d:

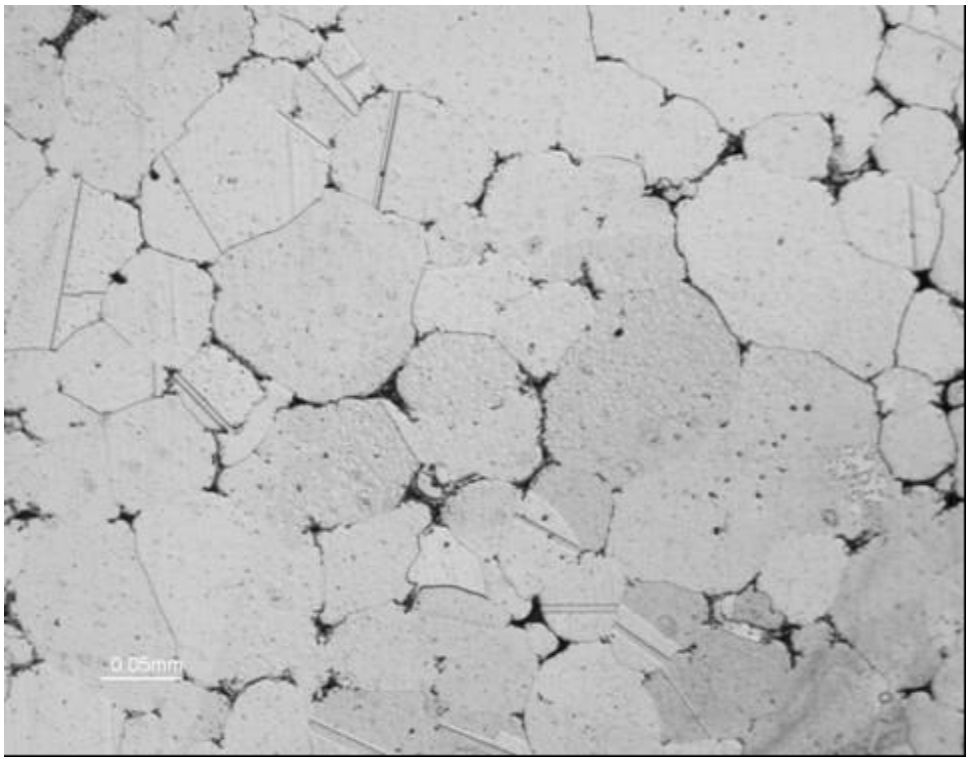

8.4 Appendix D: Mounting Directions

1. Turn the black knob on the bottom all the way to the right.

2. Pump the handle until the bottom die is visible above the sleeve.

3. Place your sample analysis side down on the die surface.

4. Turn the black knob to the left, allowing the bottom die to drop into the sleeve. Make sure it drops all the way down. If it doesn't, ask for help, don't force it.

5. Fill the die to ¼" of the threads on the inside of the sleeve with mounting powder.

6. Carefully, to avoid stripping the threads, screw the die-cap handle assembly into the top of the sleeve. Make sure you use the right one with the right die, compare serial numbers if unsure.

7. Turn the black knob all the way to the right and pump the pressure up to 4200 psi (use the 1 ¼" scale).

8. Place a heater around the outside of the die and place a thermometer into the top.

9. Heat die until the temperature is between 130 and 150 °C while keeping the pressure constant. Then hold for 1 minute.

10. Turn the heater off and remove it. Replace it with one of the cooling sleeves. Allow it to cool until 60 °C.

11. Release the pressure by turning the black knob to the left. Unscrew the die-cap handle assembly. Then turn the black knob all the way to the right to pump the bottom die above the sleeve.

12. Clean off the edges of the top and bottom dies of any flash using a pocket knife, small flat-head screwdriver or fingernail- Do not use sand paper. Also make sure there is no powder in the screw threads.

8.5 Appendix E: Directions for Programming the Furnace

3 PROGRAM DEFINITION MODE - CREATING/EDITING A PROGRAM

NOTE: Program editing/creation is not possible whilst any program is running or held.

3.1 ENTRY

In Base Mode, select the required Program Number (see Subsection 1.1), then:

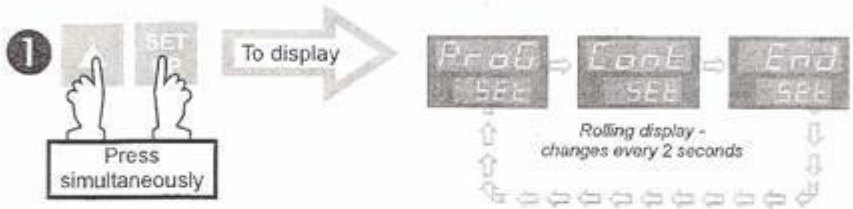

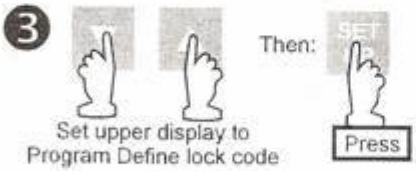

NOTE: If the Program Define Mode lock code has been set to 0, pressing the **SET UP** key in Step 2 will give direct access to Program Define Mode; no entry of lock code is required.

Upon entry into Program Define Mode, the first Segment Definition parameter for Segment 1 of the selected program will be displayed.

3-1

3.2 CREATING A PROGRAM

A program is created in two steps:

1. Define the segments of your program; the parameters used depend on what Program Mode has been configured - Rate Mode (see Subsection 3.2.2) or Time Mode (see Subsection 3.2.3). The segment definitions determine whether the selected segment is a Ramp Segment, a Dwell (soak) Segment or an End Segment.

2. Set the required Program Options (see Subsection 3.2.4). These determine:

   (i) The number of cycles performed by the program,
   (ii) The timebase to be used (hours/minutes or minutes/seconds)
   (iii) The width of the Guaranteed Soak Band (if enabled),
   (iv) The state of the event indicator for each segment in the program,
   (v) The lock code to be used for subsequent entries into Program Define Mode.

3.2.1 Basic Guidelines

1. The Controller Programmer may contain up to four programs.

2. Each program may comprise up to 16 segments.

3. Each segment may be:

   (a) a Ramp Segment (setpoint changing at a defined rate or between the initial value and a pre-determined final value over a defined time),
   (b) a Dwell Segment (setpoint constant for a defined time,) or
   (c) an End Segment (marking the end of the program).

4. A program may contain only one End Segment (the last segment in the program).

5. If the program comprises 16 segments, Segment 16 is automatically an End Segment.

3.2.2 Defining Segments - Rate Mode

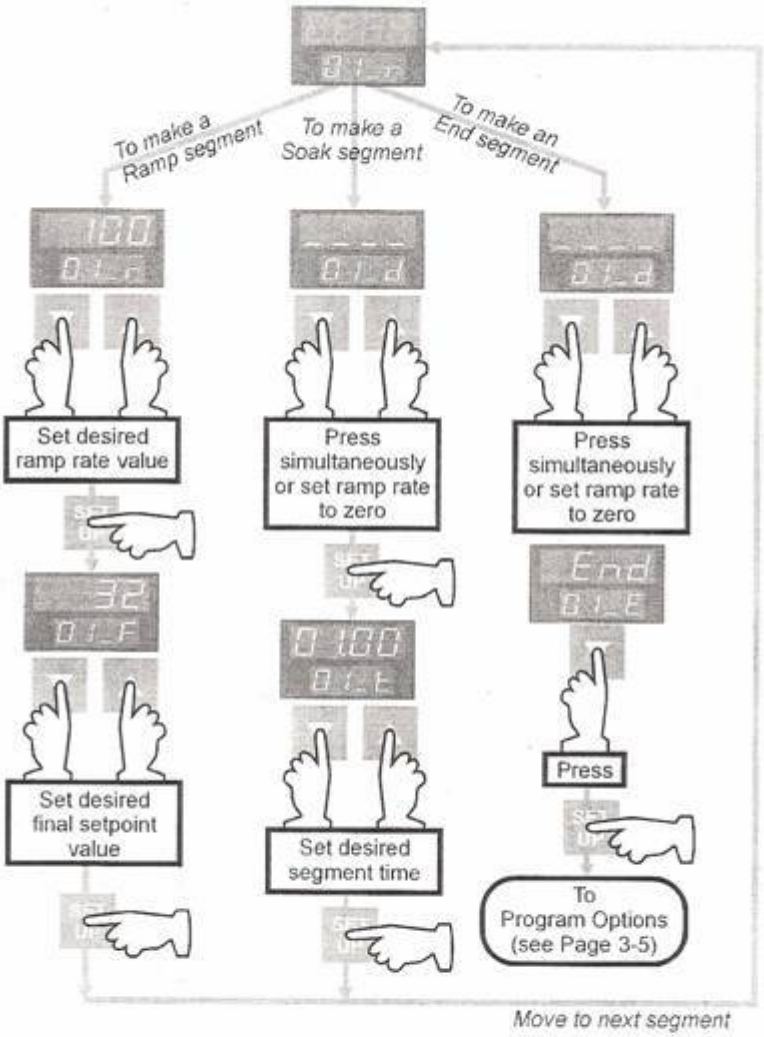

NOTE: Ramp rate is in units/hour if bASE = hour
Ramp rate is in units/minute if bASE = PM.n
} See Subsection 3.2.4

3.2.3 Defining Segments - Time Mode

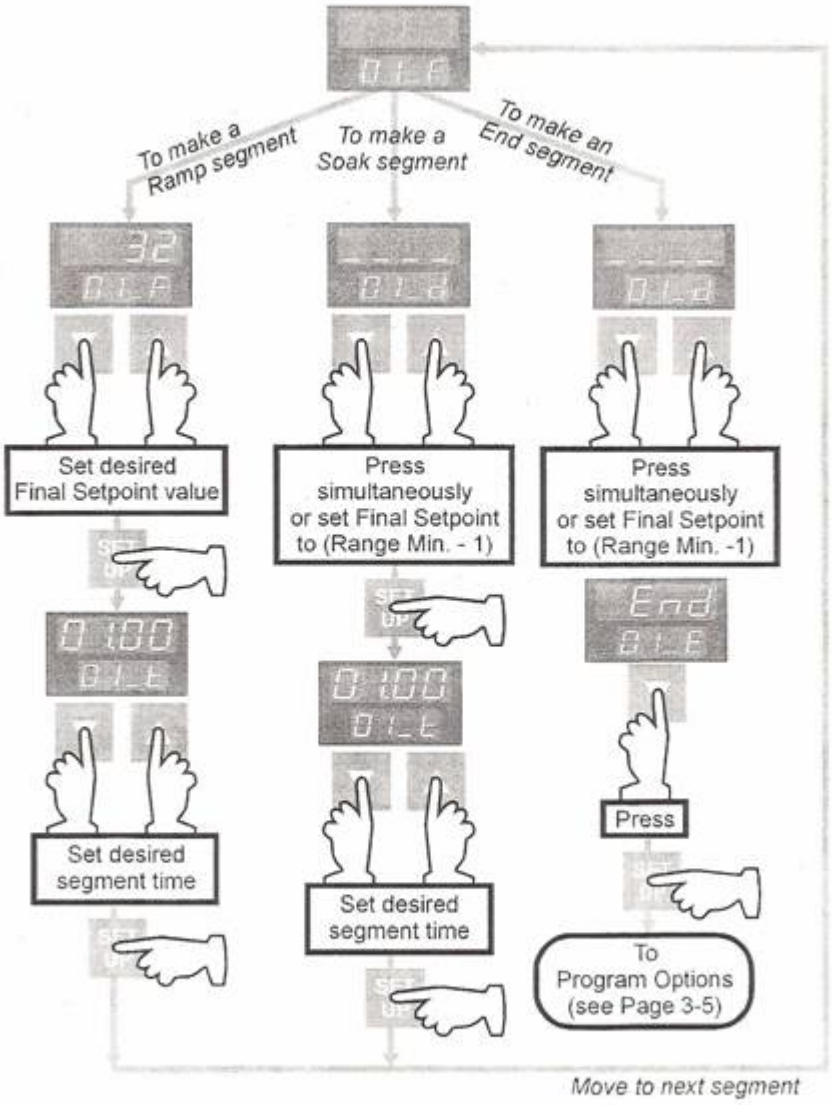

3.2.4 Program Options

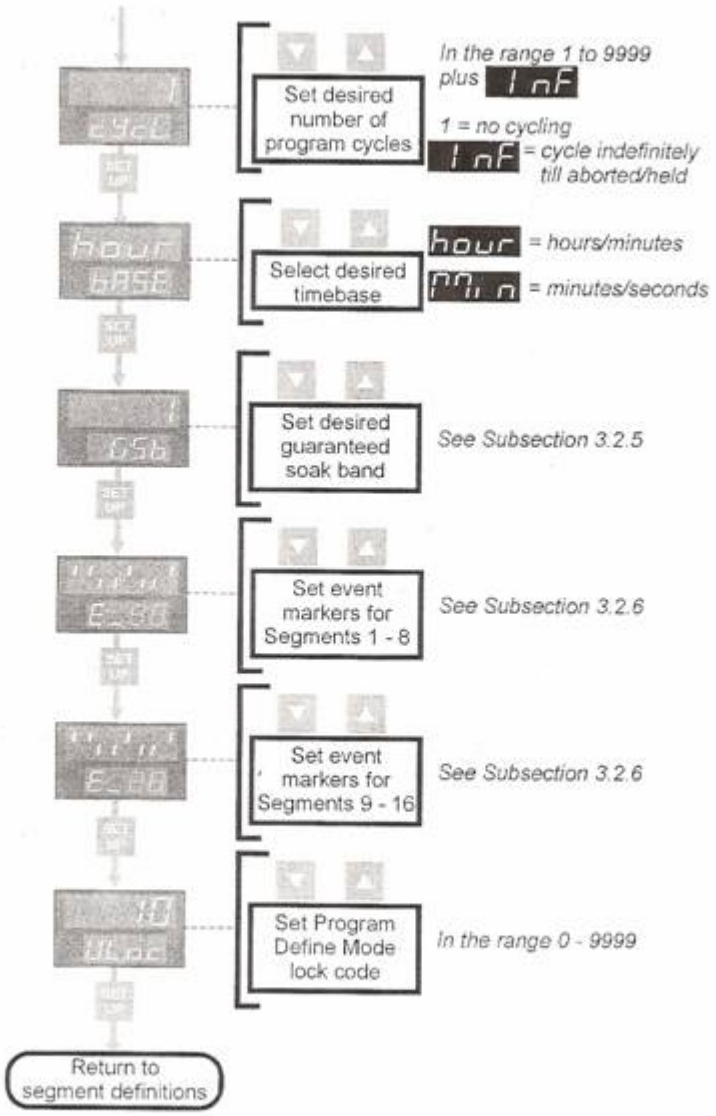

3.2.5 Guaranteed Soak Band

The Guaranteed Soak Band is applicable to sOAK segments only and operates as follows (depending on whether Guaranteed Soak has been enabled or Manual Guaranteed Soak has been configured):

GUARANTEED SOAK ENABLED

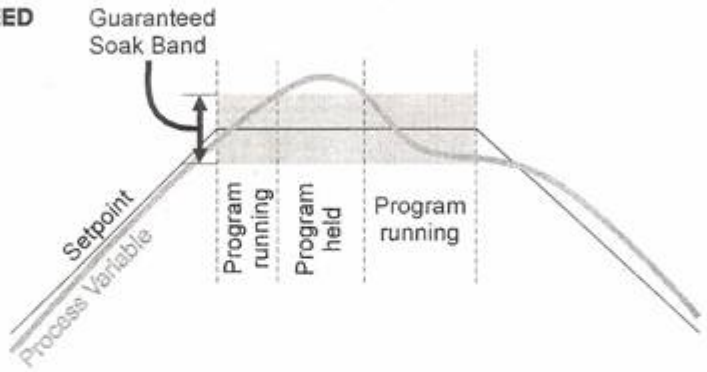

MANUAL GUARANTEED SOAK

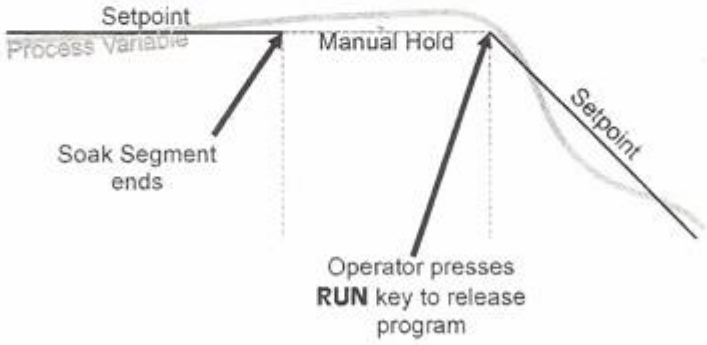

3.2.6 Segment Event Status

For every segment in a program there is an event indicator. This may be set ON or OFF for that segment. The status for the segments in the currently-selected program appears in the following form in the upper display:

DISPLAY 1

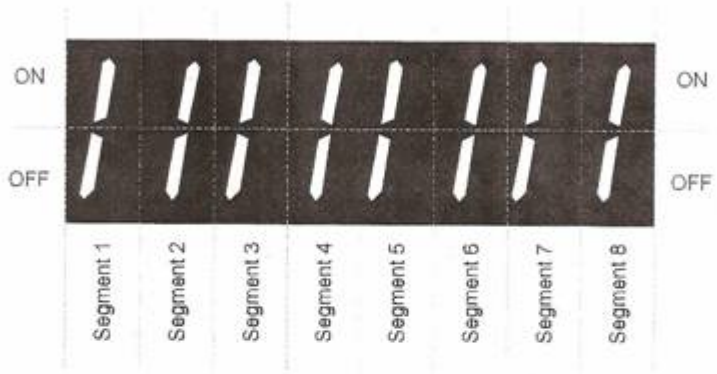

DISPLAY 2

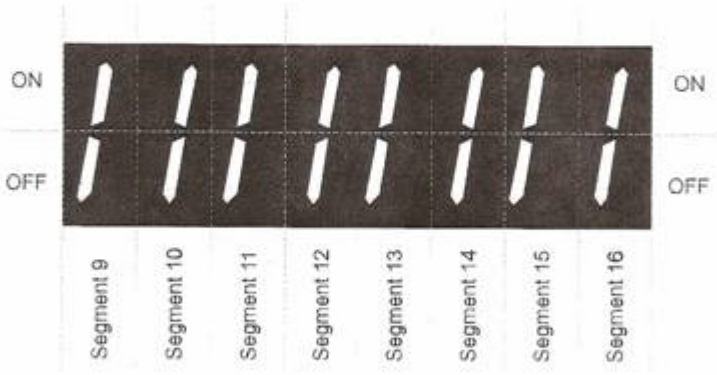

The first display shows the current event status for Segments 1 - 8 and the second display shows the current event status for Segments 9 - 16. Each event marker may be set ON (Up key) or OFF (Down key) in order of segment number. Only the event indicators for the segments in the program are displayed. If the program has less than 16 segments (including the End Segment), the non-applicable display positions are blank; if the program has eight segments or less, the second display is not

included.. The lower display shows the current segment number. Thus, the key sequence to define the event markers for Segments 1 - 8 could be:

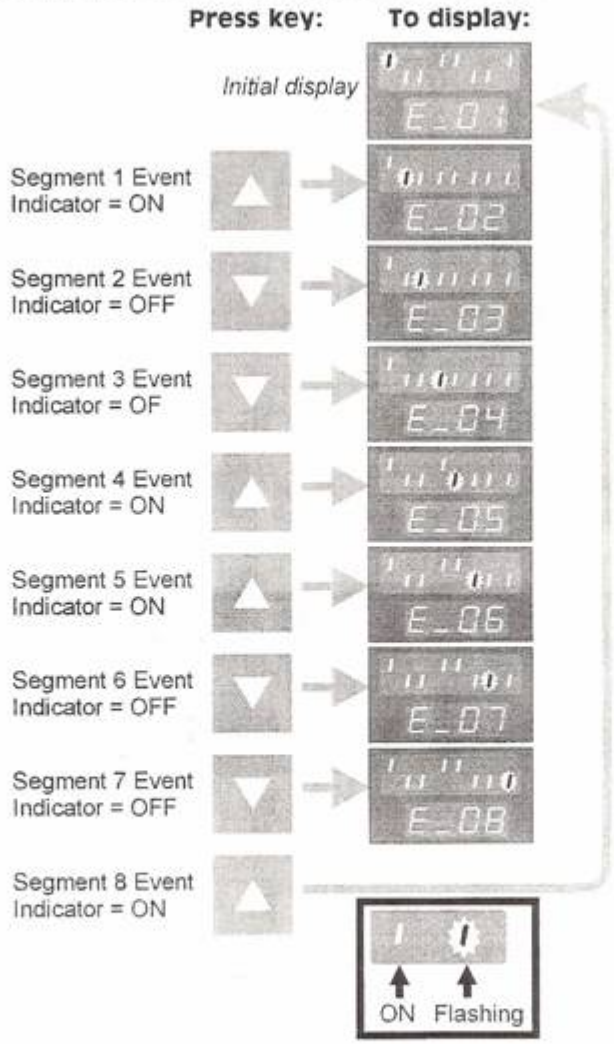

Pressing the **SET UP** key would then display the event markers for Segments 9 - 16 (as applicable), which could be defined in a similar manner.

3.3 DEFAULT VALUES AND ADJUSTMENT RANGES

Parameter	Range Minimum	Range Maximum	Default
Ramp Rate	0 = Soak segment -1 = End segment	9999, then INF	100
Final (End of Ramp) Setpoint	Range Minimum	Range Maximum	Range Minimum
Segment Time	00:00	99:59	01:00
Number of Cycles	1	9999 then INF	1
Guaranteed Soak Band	1	Span plus OFF	OFF

3.4 EXIT FROM PROGRAM DEFINE MODE

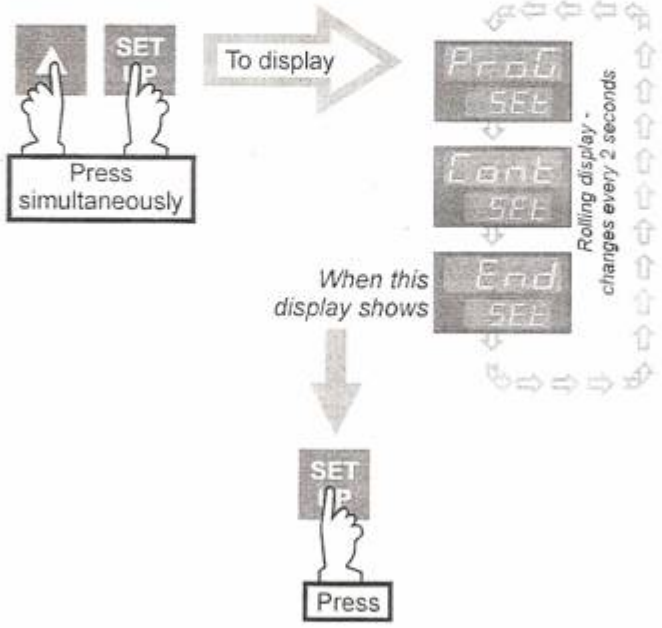

A return is then made to the normal Base Mode display.